TKK Dissertations 108
Espoo 2008

SPIN-DEPENDENT TRANSPORT IN Mn DOPED GaAs AND GaN DIODES

Doctoral Dissertation

Heikki Holmberg

Helsinki University of Technology
Faculty of Electronics, Communications and Automation
Department of Micro and Nanosciences

TKK Dissertations 108
Espoo 2008

SPIN-DEPENDENT TRANSPORT IN Mn DOPED GaAs AND GaN DIODES

Doctoral Dissertation

Heikki Holmberg

Dissertation for the degree of Doctor of Science in Technology to be presented with due permission of the Faculty of Electronics, Communications and Automation for public examination and debate in Large Seminar Hall (2190) of Micronova at Helsinki University of Technology (Espoo, Finland) on the 14th of March, 2008, at 12 noon.

Helsinki University of Technology
Faculty of Electronics, Communications and Automation
Department of Micro and Nanosciences

Teknillinen korkeakoulu
Elektroniikan, tietoliikenteen ja automaation tiedekunta
Mikro- ja nanotekniikan laitos

Distribution:
Helsinki University of Technology
Faculty of Electronics, Communications and Automation
Department of Micro and Nanosciences
P.O. Box 3500
FI - 02015 TKK
FINLAND
URL: http://www.micronova.fi/units/mns/
Tel. +358-9-451 2322
Fax +358-9-451 5008
E-mail: heikki.holmberg@tkk.fi

© 2008 Heikki Holmberg

ISBN 978-951-22-9259-2
ISBN 978-951-22-9260-8 (PDF)
ISSN 1795-2239
ISSN 1795-4584 (PDF)
URL: http://lib.tkk.fi/Diss/2008/isbn9789512292608/

TKK-DISS-2438

Multiprint Oy
Espoo 2008

ABSTRACT OF DOCTORAL DISSERTATION	HELSINKI UNIVERSITY OF TECHNLOGY P.O. BOX 1000, FI-02015 TKK http://www.tkk.fi
Author Heikki Holmberg	
Name of the dissertation Spin-dependent transport in Mn Doped GaAs and GaN diodes	
Manuscript submitted 16.11.2007	Manuscript revised 4.2.2008
Date of the defence 14.3.2008	
☐ Monograph	☒ Article dissertation (summary + original articles)
Faculty	Faculty of Electronics, Communication and Automation
Department	Department of Micro and Nanosciences, Electron Physics Group
Field of research	Semiconductor Technology
Opponent(s)	Prof. Tuure Tuuva
Supervisor	Prof. Pekka Kuivalainen

Abstract

The main idea of the thesis was to study experimentally the potential and the possibilities of semiconductor spintronic devices. Spin dependent magnetotransport was studied in different Mn doped GaAs and GaN thin films and diode structures. The ferromagnetic thin films and pn, spin Esaki-Zener tunnel and resonant tunnelling diodes were fabricated from Mn doped GaAs and GaN using the Molecule Beam Epitaxy technique. The magnetotransport measurements consist of ,e.g., *I-V*, resistance and Hall measurements as a function of magnetic field and temperature. In this study also the magnetic field dependence of the current of the ferromagnetic diodes were modeled. In addition, the material studies were carried out using Secondary Ion Mass Spectroscopy and X-ray Diffraction techniques and the magnetization measurements using a magnetometer.

The main result of this study was the observation of the tunnelling anisotropic magnetoresistance effect (TAMR) in Mn doped GaAs spin Esaki-Zener tunnel and resonant tunnelling diodes. In the Mn doped GaAs Esaki-Zener diode the TAMR effect was observed at low bias voltages, which makes it possible to fabricate ultra low power spintronic devices. Another important result was that a room temperature ferromagnet of Mn doped GaN can be fabricated by a solid state diffusion method. The effect of Mn doping on the resonant tunnelling diodes with magnetic Mn doped GaAs emitters was also characterized. In addition, the reason why the current of a pn-diode having a lightly doped region is independent of magnetic field, even when some part of the device is magnetic, is given. Also the negative magnetoresistance due to the spin disorder scattering was observed and modeled in Mn doped GaAs and GaN thin films.

Keywords : semiconductor, spintronics, tunneling, diode, magnetotransport, Mn, GaAs, GaN			
ISBN (printed)	978-951-22-9259-2	ISSN (printed)	1795-2239
ISBN (pdf)	978-951-22-9260-8	ISSN (pdf)	1795-4584
Language	English	Number of pages	59+app. 51
Publisher	Helsinki University of Technology, Department of Micro and Nanosciences		
Print distribution	Helsinki University of Technology, Department of Micro and Nanosciences		
☒ The dissertation can be read at http://lib.tkk.fi/Diss/2008/isbn9789512292608/			

VÄITÖSKIRJAN TIIVISTELMÄ	TEKNILLINEN KORKEAKOULU PL 1000, 02015 TKK http://www.tkk.fi
Tekijä Heikki Holmberg	
Väitöskirjan nimi Spinistä riippuva sähkönkuljetus Mn seostetuissa GaAs ja GaN diodeissa	
Käsikirjoituksen päivämäärä 16.11.2007	Korjatun käsikirjoituksen päivämäärä 4.2.2008
Väitöstilaisuuden ajankohta 14.3.2008	
☐ Monografia	☒ Yhdistelmäväitöskirja (yhteenveto + erillisartikkelit)

Tiedekunta	Elektroniikan, tietoliikenteen ja automaation tiedekunta
Osasto	Mikro- ja Nanotekniikan osasto, Elektronifysiikan ryhmä
Tutkimusala	Puolijohdeteknologia
Vastaväittäjä(t)	Prof. Tuure Tuuva
Työn valvoja	Prof. Pekka Kuivalainen

Tiivistelmä

Väitöskirjan päätavoite oli kokeellisesti tutkia puolijohdespintroniikkakomponenttien potentiaalia ja mahdollisuuksia. Työssä tutkittiin spinistä riippuvaa sähkönkuljetusta erilaisissa Mn:lla seostetuissa GaAs ja GaN ohutkalvoissa ja diodirakenteissa. Työssä valmistettiin molekyylisuihkuepitaksia menetelmän avulla ferromagneettisia ohutkalvoja, pn-diodeja, spin Esaki-Zener tunneli-diodeja ja resonanssitunnelidiodeja Mn:lla seostetuista GaAs:sta ja GaN:sta. Galvanomagneettiset mittaukset koostuivat mm. virta-jännite, resistanssi- ja Hall-mittauksista magneettikentän ja lämpötilan funktiona. Tutkimuksessa myös mallinnettiin ferromagneettisten diodien havaittuja virran magneettikenttäriippuvuuksia. Lisäksi näytteille tehtiin materiaalitutkimuksia SIMS- ja XRD-menetelmillä ja magnetointimittauksia magnetometrillä.

Tutkimuksen päätulos oli tunnelivirran voimakkaan magneettikenttäriippuvuuden ns. TAMR (Tunnel Anisotropic Magnetoresistance) havaitseminen ferromagneettisessa Mn seostetussa GaAs spin Esaki-Zener tunneli- ja resonanssitunnelidiodeissa. TAMR ilmiö havaittiin Mn:lla seostetuissa GaAs Esaki-Zener diodeissa pienillä bias-jännitteillä, joka tekee mahdolliseksi erittäin pienen tehonkulutuksen omaavan spintroniikkakomponentin valmistamisen. Toinen merkittävä tulos oli, että tutkimuksessa onnistuttiin valmistamaan diffuusion avulla Mn seostutettuja GaN ohutkalvoja, jotka ovat ferromagneettisia huoneenlämpötilassa. (Ga,Mn)As resonanssitunnelidiodin virran riippuvuutta Mn seostuksesta tutkittiin. Lisäksi työssä selitettiin, miksi heikosti seostetun pn-diodin virta ei riipu magneettikentästä, vaikka jokin pn-diodin osa olisi magneettinen. Mn seostetuissa GaAs ja GaN ohutkalvoissa havaittiin myös spin-epäjärjestys sirontaa ja negatiivista magnetoresistanssia.

Asiasanat	Puolijohde, spintroniikka, tunnelointi, diodi, galvanomagneettisuus, Mn, GaAs, GaN
ISBN (painettu) 978-951-22-9259-2	ISSN (painettu) 1795-2239
ISBN (pdf) 978-951-22-9260-8	ISSN (pdf) 1795-4584
Kieli Englanti	Sivumäärä 59+liit. 51
Julkaisija	Teknillinen korkeakoulu, Mikro- ja nanotekniikan laitos
Painetun väitöskirjan jakelu	Teknillinen korkeakoulu, Mikro- ja nanotekniikan laitos
☒ Luettavissa verkossa osoitteessa http://lib.tkk.fi/Diss/2008/isbn9789512292608/	

Preface

The work was carried out at the Electron Physics Group in the Micro and Nanosciences laboratory during 2003-2007. The thesis was part of the project “Room temperature spintronics” and was funded by the Academy of Finland. The author got funding from the Graduate School of the Electrical and Communications Engineering department (HUT), the Finnish Technology Foundation, the Foundation of Emil Aaltonen and the Foundation of Electronics Engineers.

I want to express my gratitude to the supervisor of this thesis, Pekka Kuivalainen who has given me a lot of excellent advice and guidance for my thesis. I also want to thank Sergey Novikov for fabricating the samples and giving hints related to the measurement system. In addition, I am also grateful to Natalia Lebedeva for helping with measuring some of the samples used in this study. Of course, I would like to thank all the staff of the Electron Physics Group for a great working environment. Charlotta Tuovinen has been a great help with checking the English spelling of this thesis. I am also very grateful to pre-examiners Dr. Jari Paloheimo and Dr. Jouni Ahopelto who have both provided me with valuable comments and suggestions for improvements.

Last, but not least, I am very grateful to my parents Harri and Pirjo for their mental and financial support throughout my studies. In addition, I would also like to thank my brother Ilkka and my sister Heidi for their encouragement and support during my studies.

Heikki Holmberg

Espoo 16.11.2007

Contents

Preface **7**

Contents **8**

List of Publications **10**

Author's contribution **11**

List of Abbreviations **12**

List of Symbols **13**

1. Introduction **16**

2. Diluted Magnetic Semiconductor (DMS) **19**

2.1. Mn Doped GaAs 21

2.2. Mn Doped GaN 21

2.3. Metal-Insulator- Transition in DMS 22

2.4. Magnetoresistance in DMS 23

3. Modeling of Magnetic Diodes **26**

3.1. Modeling of the Magnetic Pn-diodes 26

3.2 Modeling of the Resonant Tunnelling Diode (RTD) with a Ferromagnetic Emitter 28

4. Experimental Techniques and Fabrication of the Magnetic Thin Films and Diodes **31**

4.1 Molecular Beam Epitaxy 31

4.2 Fabrication of Mn Doped GaAs Thin Films and Diodes 33

4.2.1 Mn doped GaAs Thin Films 33

4.2.2 Mn Doped GaAs Pn-diodes 33

4.2.3 Magnetic RTD with Magnetic Emitter 34

4.3 Mn Doped GaN Thin Films and Pn-diode 34

4.3.1 Mn Doped GaN Thin Films 34

4.3.2 Mn Doped GaN Pn-Diode 35

5. Results 36

5.1 Magnetic Mn Doped GaAs Thin Films 36

5.2 Magnetic Mn Doped GaAs Pn-diodes 37

5.3 Magnetic RTD with Magnetic Emitter 43

5.4 Results of Mn doped GaN Layers and Pn-diodes 47

6 Future Prospect 53

7 Summary 55

References 57

List of Publications

This thesis consists of an overview and of the following publications which are referred to in the text by their Roman numerals.

I H. Holmberg , N. Lebedeva, S. Novikov, J. Ikonen, P.Kuivalainen,M. Malfait and V. Moschchalkov, *Large magnetoresistance in a ferromagnetic GaMnAs/GaAs Zener-diode,* Europhysics Letters **71** (5), 811-816 (2005)

II H.Holmberg, N.Lebedeva, S.Novikov, P.Kuivalainen, M.Malfait, V.V Mohschalkov and P. Kostamo, *Magnetotransport properties of Room Temperature Ferromagnet (Ga,Mn)N,* IEEE Transactions on Magnetics **41** (10), 2736-2738 (2005)

III H.Holmberg, N.Lebedeva, S.Novikov, P.Kuivalainen, M.Malfait and V.V Moschalkov, *Magnetotransport in ferromagnetic (Ga,Mn)As and (Ga,Mn)N pn-diodes,* IEEE Transactions on Magnetics **42,** 2712-2714 (2006)

IV H.Holmberg, N.Lebedeva, S.Novikov, P.Kuivalainen, M.Malfait, and V.V.Moshchalkov *Electrical transport in Mn-doped GaAs pn-diodes.* Physica Status Solidi (a) **204** (3), 791-804 (2007)

V H.Holmberg, N. Lebedeva, S.Novikov, M.Mattila, P.Kuivalainen, G.Du, X.Han, M.Malfait, and V.V. Moshchalkov; *Magnetotransport of holes through an AlAs/GaAs/AlAs resonant tunnelling quantum well with a ferromagnetic* $Ga_{1-x}Mn_xAs$ *emitter*, Physica Status Solidi (a) **204** (10), 3463-3477 (2007)

Author's contribution

All magnetotransport characterization of the magnetic thin films and magnetic diodes were planned and carried out by the author with help for the measurements from M. Sc. N. Lebedeva in the case of the Publication I. The magnetotransport characterization included e.g. Hall measurements, *I-V* curve measurements, and sheet resistance measurements as a function of temperature and magnetic field. The growth parameters and the sample and device structures for all publications were designed by the author together with Dr. Sergey Novikov. All samples were grown by Dr. Sergey Novikov (using MBE) except the non- magnetic RTD structures, which were grown by Dr. Marco Mattila (using MOVPE). The author has written the first version of the manuscripts for Publications I, II, and III and he is the main author of them. The author has actively participated the writing of the manuscripts of Publications IV-V and is the also the main author of those publications. In addition, the author has actively contributed to the modeling and the analysis of the data in all the publications. The direct magnetization measurements in all publications were done by Dr. Malfait. In Publication II the XRD measurements was performed by M. Sc. P. Kostamo and the SIMS measurements by Dr. Likonen (VTT).

In addition, the author has presented the result of the work at major international conferences including the IEEE International Magnetics Conference (INTERMAG) 2005 in Nagoya (Japan) and INTERMAG 2006 San Diego (USA).

List of Abbreviations

DH-model	Dubson-Holcomb model
DOS	Density of States
DMS	Diluted Magnetic Semiconductor
GMR	Giant Magnetoresistance Effect
HH	Heavy Hole
LH	Light Hole
MBE	Molecular Beam Epitaxy
MIT	Metal-Insulator-Transition
MOVPE	Metal-Organic Vapor Phase Epitaxy
MR	Magnetoresistance
MRAM	Magnetic Random Access Memory
RTD	Resonant Tunnelling Diode
SIMS	Secondary Ion Mass Spectroscopy
TMR	Tunnelling Magnetoresistance
TMR^J	Tunnelling Magnetoresistance based on Julliere formula
TAMR	Tunnelling Anisotropic Magnetoresistance
UHV	Ultra High Vacuum
XRD	X-ray Diffraction

List of Symbols

A	Area
a_0	Lattice constant
B	Magnetic Field
C	Constant
$D_C(E)$	Density of states for the conduction band
$D_V(E)$	Density of states for the valence band
$D_{n\downarrow(\uparrow)}$	Diffusion constant for spin down (up) electrons
D_p	Diffusion constant for holes
E	Energy
E_σ^{res}	The energy of the resonant level
E_C	Energy of the conduction band maximum
E_F	Fermi energy
$E_{F\sigma}^{L(R)}$	Fermi energy of the spin-polarized subband on the left (right) side of a RTD
$E_{F0}^{L(R)}$	Quasi-Fermi level of the holes before the band splitting on the left (right) side of a RTD
E_m	Mobility edge
E_V	Energy of the valence band minimum
$f_C(E)$	Occupation probabilities for the conduction
$f_v^\sigma(E)$	Occupation probabilities for valence bands
$\hbar$	Planck constant
H_{ex}	Heisenberg Hamiltonian
I_{diff}	Diffusion current
I_{rec}	Recombination current
I_{tot}	Total current
I_{tunn}	Tunnelling current
I_V	Valley current related to the excess current in pn-diode
I_x	Excess tunnelling current
J_{exch}	Exchange coupling parameter

J_{pd} p-d exchange coupling parameter

$J_T^{\uparrow(\downarrow)}$ Tunnelling current for spin up electrons (spin down)

k_B Boltzmann constant

$L_{n\downarrow(\uparrow)}$ Diffusion length for spin down (up) electrons

L_p Diffusion length for holes

M_C Number of equivalent minima in conduction band

$m_{de(dh)}$ Density of state effective mass for the electron (holes)

m_r^* Electron-hole reduced mass

m_0 Rest mass of the electron

N_A Acceptor doping concentration

N_D Donor doping concentration

N^* Reduced doping concentration

n Electron concentration

n_i Intrinsic carrier concentration

$P_{L(R)}$ Polarization on the left (light) side of the sample

p Hole concentration

p_1 Parameter related to the energy dependence of energy band

p_2 Parameter related to the energy dependence of energy band

q Electron charge

R_{AP} Resistance at antiparallel spin-orientation

R_P Resistance at parallel spin-orientation

S Spin

$\vec{S}_i$ Total spin of a magnetic atom at the site *i*

$S_\sigma(E)$ The supply function

$\vec{s}$ Charge carrier spin

T Temperature

$T_{\uparrow(\downarrow)}(E)$ Quantum mechanical transmission coefficient through the double barrier

T_C Curie temperature

V Voltage

V_V Valley voltage related to the excess current in pn-diode

V_{QW}	Voltage related to the Quantum Well in RTD
x	Mole fraction
$\frac{dV}{dI}$	Conductance
$\delta_{\sigma\downarrow(\uparrow)}$	Dirac's delta function
ε_S	Dielectric constant for semiconductor
Δ	Band splitting parameter
$\rho_{DH}(T)$	The resistivity according to Dubson-Holcomb model
ρ_{300}	The resistivity at 300 K
ρ_s	Resistivity caused by spin-disorder scattering
ρ_0	Prefactor of the resistivity
$\langle S^z \rangle$	Average spin polarization of magnetic ions
Γ	Spin-independent full width of the half-maximum of the resonance
$\Gamma_{L(T)}$	The partial width of Γ for the left (right barriers)

1. Introduction

Spintronics, which is a new emerging field of nanoelectronics, is based on the utilization of electron spin in addition to its charge. By exploiting the properties of electron spin, totally new features such as multifunctional devices can be added to conventional electronics [1]. Additionally, spintronic devices will consume less energy than devices based on electron charge since the energy needed to change the orientation of spin is much smaller than the one typically required in charge transport [1].

In the mid 1930's Mott postulated his famous two-current model [2] and this can be considered the starting point of the development of spintronics. However, the actual breakthrough happened in 1988 when independently Fert et. al. [3] and Grünberg et. al. [4] discovered the Giant Magnetoresistance effect (GMR) in thin ferromagnetic metallic superlattices. Both Grünberg and Fert got the 2007 Nobel Prize in Physics for their findings. Their discovery launched a rapid development of spintronics which led to commercial success. In less than 10 years the first read head for computer hard drives based on the GMR effect was put on the market by IBM. The research, which made this fast development possible, was mainly carried out by Parkin's research group [5-7] at IBM. Nowadays almost all computer read heads are based on the GMR effect. Also new spintronic memory applications have been studied, such as the Magnetic Random Access Memories (MRAM), which are based on magnetic tunnel junctions [8].

All the current commercial spintronic applications are based on magnetic metals but semiconductor spintronics offers some advantages compared to magnetic metals [8]. Firstly, it is easier to integrate semiconductor spintronic devices with conventional electronics. Secondly, since in many magnetic semiconductors the magnetism is carrier mediated, the magnetism can be controlled by changing the bias voltage. In addition, some magnetic phenomena are stronger in semiconductors than in metals, e.g, in general the spin polarization is larger in semiconductors than in metals and signal amplification is possible in semiconductor spintronics.

Semiconductor spintronics was studied already in the 1960's. Back then the research was focused mainly on europium and chromium chalcogenide compounds (e.g. EuO, EuSe, and $CdCr_2S_4$) [9]. However, the ferromagnetic ordering temperature (=Curie temperature) T_c of those compounds was typically below 100 K. In addition, it was extremely difficult to fabricate those compounds. In the late 1980's the breakthrough of semiconductor spintronics occurred when it was discovered that adding a small amount of magnetic impurities into III-V compound semiconductors makes the compounds ferromagnetic. These compounds are called diluted magnetic semiconductors (DMS). The first actual ferromagnetic DMS structure was fabricated by Munekata's group [10]. They successfully fabricated ferromagnetic Mn doped InAs thin films on top of GaAs substrate.

The main problem with DMS is to find a suitable material combination that is compatible with conventional semiconductor technology and simultaneously has a Curie-temperature above room temperature. The research has been focused on Mn doped InAs, GaAs and GaN. All those compounds have great advantages but unfortunately also some disadvantages. The physical properties of the compound semiconductors are described in more detail in Chapters 2.1 and 2.2. Recently many research groups have started to fabricate and study also actual spintronic devices. Currently ferromagnetic pn-diodes, Spin Esaki-Zener tunnel-diodes, Schottky-diodes and resonant-tunnelling diodes, have been fabricated (See Ref. [11] and the reference therein). A more detailed description of spintronic devices can be found in Chapter 5 of the present overview.

This overview and publications focus on the characterization of the magnetic diodes fabricated of Mn doped GaAs and Mn doped GaN. At the beginning of this thesis the special properties of DMS are briefly introduced. Then the theory of some spintronic semiconductor devices is presented in Chapter 3. The fabrication processes of these devices as well as the measurement techniques are described in Chapter 4. In Chapter 5 of this overview the most important experimental results are shown and explained. The future prospects are discussed in chapter 6. Finally, a summary is given in Chapter 7.

Publication I deals with the characterization of the magnetotrasport properties of magnetic Spin Esaki-Zener tunnel-diodes. In this publication, the tunnelling anisotropic magnetoresistance (TAMR) is observed for the first time in a tunnel diode. In Publication II the properties of a room temperature Mn doped GaN ferromagnet are presented. The method used for fabricating the Mn doped GaN was solid state diffusion. The solid state diffusion method is quite a simple and cheap fabrication method. Mn doped GaAs and GaN pn-diodes are studied in Publication III. In publication III one of the first spintronic devices of Mn doped GaN was actually fabricated. In Publication IV various ferromagnetic GaAs pn-diodes are studied. Especially, the effect of ferromagnetism on *I-V* characteristics in pn-diodes are studied and explained in detail. In addition to the experimental results, also the question of what are the conditions when the *I-V* characteristics are magnetic field dependent is answered. Finally, the resonant tunnel diodes (RTDs) with magnetic emitters are studied in Publication V. In that article the effect of the doping level of emitter on the magnetic field dependence of I-V characteristics is studied. The most important result was the observation of the TAMR effect for the first time in RTDs.

2. Diluted Magnetic Semiconductor (DMS)

In diluted magnetic semiconductors the magnetism is achieved by doping a small amount of magnetic atoms into a non-magnetic semiconductor. In the ideal case, the magnetic atoms randomly replace some of the lattice atoms of the non-magnetic host material. The most common doping atom is Mn, but also Cr and Fe are widely used [9]. The reason for using Mn is the fact that it has five unpaired electrons in the d-shell, and therefore its total spin has a large value S=5/2 [12]. Depending on the doping level and the distance between the doping atoms, DMSs may exhibit para-, ferro- or antiferromagnetic behavior. The electrical transport properties of DMSs also depend on the doping level and therefore the properties vary between insulating and metallic behavior.

The first ferromagnetic III-V compound semiconductor, Mn doped InAs was fabricated by Munekata's group [10] in 1989. In 1992 Ohno et. al. [13] discovered that the ferromagnetism in p-type Mn doped InAs is hole-induced. The next major step in semiconductor spintronics was made when two groups were able to fabricate ferromagnetic p-type Mn doped GaAs [14-15]. After that Dietl presented the theory of Mn doped GaAs and showed that the ferromagnetism in Mn doped GaAs is free carrier induced [16]. His theory also suggests that by doping the GaAs more heavily the Curie-temperature should increase. However, so far the increase of the Curie temperature of Mn doped GaAs has been saturated at 173 K [17]. Nazmul et. al. [18] have proposed that by a δ doping of Mn combined with a p-type modulation of the sample the Curie-temperature can be increased even to 240 K. However, the commercial applications require higher Curie temperatures (T_C>300K) and therefore further research is still needed.

When it became obvious that it would be difficult to obtain room temperature ferromagnetism in Mn doped GaAs, other materials were studied. The theoretical calculations by Dielt [19] predicted that, e.g, Mn doped GaN could be ferromagnetic even at room temperature. Indeed, during the last few years many groups have reported

room temperature ferromagnetism in Mn doped GaN [20-23]. However, the ferromagnetism in those structures could not be explained by Dietl's model and the real reason for ferromagnetism in III-V wide-band DMS is still uncertain to some extent. The problem is related to the fact that the Mn acceptor energy level in GaN is not close to the valence band edge and therefore it is difficult to obtain a high carrier concentration, which is needed for carrier induced ferromagnetism. In closer examination of the Mn doped GaN samples it has been observed that the Mn atoms are not distributed spatially homogeneously. The Mn in those samples is either in small nanoclusters or it forms some compounds with N.

The coupling between the electrical and magnetic properties in DMSs occurs because there is an exchange interaction between the total spin of a magnetic atom $\vec{S}$ at the site i and the charge carrier spin $\vec{s}$. This interaction can be described by a Heisenberg exchange coupling model

$$H_{ex} = -J_{pd} \sum_i \vec{s} \bullet \vec{S}_i \ , \tag{1}$$

where J_{pd} is the exchange coupling parameter. The interaction (1) causes a spin splitting of the energy levels of the charge carriers ,i.e., spin up and spin down bands are formed. The energy difference between the spinpolarized subbands, the so-called band splitting parameter, is given by

$$\Delta = xJ_{pd} \left\langle S^z \right\rangle \tag{2}$$

where x is the mole fraction of Mn ions and $<S^z>$ is the average spin polarization of magnetic ions. The band splitting parameter Δ is one of the most important model parameters in the modeling of the new spintronic devices [24]. The interaction (1) also causes additional scattering of the charge carriers due to the large spin fluctuations in the magnetic subsystems, especially at $T \approx T_C$. The spin disorder scattering is manifested as a resistivity peak at $T = T_C$ [24] .

2.1. Mn Doped GaAs

Mn doped GaAs is the most studied III-V DMS material so far [25]. The origin of ferromagnetism in Mn doped GaAs is quite well understood and it can be explained qualitatively and in many cases also quantitatively by the p-d Zener model described by Dielt[19]. The theory is based on a model proposed by Zener for magnetic metals [26]. However, the model was later abandoned due to the development of more accurate models for metals, i.e. the RKKY model. The main finding in Dietl's model is that ferromagnetism in Mn doped GaAs is mediated by holes.

In the ideal case every Mn atom will replace a Ga atom in the GaAs lattice, which increases the hole concentration of the sample. However, it has been observed that the hole concentration is smaller than the amount of the Mn atoms doped in the GaAs. This is due to two factors. Firstly, in the growth process some As atoms will replace Ga atoms, which will then decrease the hole concentration since As belongs to atoms of group V. Secondly, some of the Mn atoms will be in interstitial sites on the lattice. In addition, the electronic configuration of the Mn atoms in GaAs has been proven to be d^5+h [27], and the acceptor level of the Mn-atoms is about 110 meV above the edge of the valence band [28].

Also the spin orientation related phenomena have been studied. A spin polarization of 80% in Mn doped GaAs has been measured using Andreev reflection [29], which is sufficient for practical applications. Also giant magnetoresistance (GMR) [30], tunnelling magnetoresistance (TMR) [31] and tunnelling anisotropic magnetoresistance (TAMR) [32] have been observed in Mn doped GaAs layers.

2.2. Mn Doped GaN

GaN is a commonly used material in optoelectronics, and therefore its properties are quite well known. GaN, as well as GaAs, is a direct band gap material, but the forbidden energy gap of GaN is much larger than that of GaAs. The interest in Mn doped GaN increased rapidly, when Dietl predicted that Mn doped GaN should be ferromagnetic even at room temperature, based on his p-d Zener model [19].

The origin of ferromagnetism in Mn doped GaN is still unclear. Many models have been proposed [33-36], but none of the models have been fully verified by measurements. Dietl's model as such cannot be applied to Mn doped GaN since the Mn energy level in the GaN bandgap is 1.8 eV [37] above the valence band and therefore the hole concentration cannot be very high in the case of Mn doping [33]. An additional interesting fact is that n-type Mn doped GaN with high T_C has been found e.g. [Publication II] [38]. The suggested reason for this is that the growth conditions of the sample may cause the sample to change from p-type to n-type [39]. A more detailed description of different models can be found in a review article [40].

Despite the theoretical difficulties, many groups have experimentally observed ferromagnetism even at room temperature in Mn doped GaN [20-23]. The contradictory experimental results are mainly due to Ga,Mn and N forming additional different compounds in Mn doped GaN [41]. There is still no clear evidence that the structure of Mn doped GaN would be same as Mn doped GaAs, i.e. the spatially distributed DMS structure. On the contrary, it seems that samples that exhibit room temperature ferromagnetism are either formed of nanoclusters or the Mn has formed some other compound with N and Ga than (Ga,Mn)N [41-42]. The exact identification of small nanoclusters is not easy, and it causes difficulties in the interpretation of the results. The different experimental results indicate that there might be several different mechanisms behind the ferromagnetism in Mn doped GaN, and therefore it is important to continue the material studies.

2.3. Metal-Insulator- Transition in DMS

The electrical transport properties of the ferromagnetic DMSs can vary between metallic and insulating behavior. The metal-insulator-transition (MIT) depends on the carrier concentration of the sample. In doped non-magnetic semiconductor the MIT occurs when the ratio of the average distance between the carriers r_c is about 2.4 times the effective Bohr radius [43].

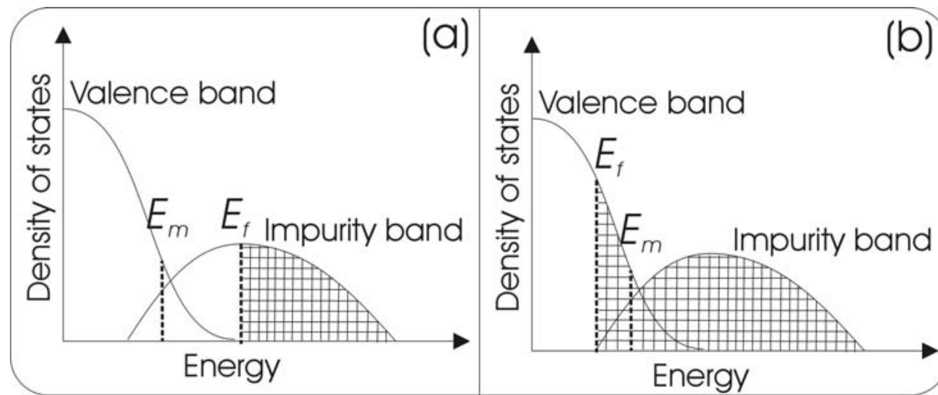

Fig. 1. *Schematic figure of the band structure in the Mn doped GaAs: a) insulating material b) metallic material. The shaded areas are occupied states (holes). E_m is the mobility edge, which separates the extended and localized electronic states.*

When the ferromagnetic DMS is on the metallic side of the transition, the Fermi-level of the DMS is in the extended band states above the mobility edge E_m and in the insulator region the Fermi-level is in the localized region (Fig.1.). The conduction mechanisms are not the same on the different sides of the transition. The conduction of the insulator (or the semiconductor) is due to carrier hopping between the localized states, and therefore the conduction decreases as a function of temperature at low temperatures. On the metallic side of the MIT the conduction is metallic and it approaches a finite value even at absolute zero temperature [44].

2.4. Magnetoresistance in DMS

The normal magnetoresistance (MR) for free carriers in valence and conduction bands in non-magnetic semiconductors typically depends on the absolute value of the square of the magnetic field [45] and the MR is positive. In DMS the situation is different due to spin disorder scattering, which increases the resistivity at $T \approx T_C$. On the other hand the external magnetic field decreases the spin fluctuations, and consequently the resistivity. Therefore in ferromagnetic DMS the magnetoresistance is negative.

A structure of a very thin non-magnetic layer between two thin ferromagnetic metal thin films can have a large magnetoresistance. This phenomenon is called the giant magnetoresistance effect (GMR). Almost all commercial spintronic devices are based on that phenomenon ,e.g., read heads for computer hard drives. However, if the non-

magnetic layer between the two ferromagnetic layers is replaced with a very thin insulating layer, we have a magnetic tunnelling junction instead of GMR structure. The tunnelling through the thin insulator also layer depends on the spin orientation. The tunnelling magnetoresistance is defined as

$$TMR = \frac{R_{AP} - R_P}{R_{AP}}, \quad (3)$$

where R_{AP} is the resistance, when the spins of the ferromagnetic layers have antiparallel orientations and R_P is the resistance when the spins are parallel. The TMR has even larger magnetoresitance than GMR [46]. If it is assumed that spin is conserved in the tunnelling process, it leads to the well known Julliere formula [47]

$$TMR^J = \frac{2P_L P_R}{1 + P_L P_R}, \quad (4)$$

where P_L and P_R are the polarizations of the left and right sides of the sample, respectively. However, the Julliere formula cannot explain the tunnelling magnetoresistance in Mn doped GaAs structures [48], where the TMR depends also on the angle between the magnetization and the current. This phenomenon is called the tunnelling anisotropic magnetoresistance (TAMR). It cannot be observed in magnetic metals due to the small spin-orbit coupling in metals.

TAMR is due to the strong spin-orbit coupling, the highly anisotropic Fermi-level surface in (Ga,Mn)As [49] and large exchange coupling between delocalized holes and localized magnetic Mn impurities [50]. All of these cause additional unaxial anisotropic changes to the densities of states (DOS) in the valence band of the Mn doped GaAs. On the other hand, the tunnelling current is proportional to the DOS, and therefore also the magnetoresistance depends on the angle between the magnetization and the tunnelling current.

The TAMR effect has many interesting properties that can be used in new spintronic devices. One of the greatest advantages of TAMR over TMR is that the TAMR effect does not require multilayer structures [51-52]. Another great benefit of TAMR is that it is almost independent of the spin flip processes during the tunnelling process.

Furthermore, depending on bias conditions TAMR can be either negative or positive [32]. TAMR can be used to design a low power spintronic device, since the TAMR effect can be observed at really small bias voltages. In addition, in ferromagnetic thin films the orientation of the magnetization of the sample can be changed continuously and reversibly if the direction of the applied magnetic field and the easy axis of the magnetization of the sample are correctly chosen.

3. Modeling of Magnetic Diodes

After the discovery of ferromagnetism in III-V DMS thin films, it was obvious that also various device structures based on those materials should be tested, both by modeling and by fabricating. Many groups have proposed different kind of spintronic transistors and diodes. Many of those devices have been fabricated and studied, such as magnetic pn-diodes, Schottky diodes, and RTD diodes [11]. However, many of the proposed devices, in particular transistors such as the Datta-Das spin field-effect transistor based on the Rashba effect (spin-orbit interaction) [53] have not yet been successfully fabricated.

3.1. Modeling of the Magnetic Pn-diodes

The exchange interaction (1) causes band splitting and spin-disorder scattering, which have an effect on the *I-V* characteristics of the magnetic pn-diodes [54]. The total current of a magnetic pn-diode is given by

$$I_{tot} = I_{diff} + I_{rec} + I_{tunn} + I_X \ , \tag{5}$$

where I_{diff} is the diffusion current, and I_{rec} is associated with the recombination processes in the depletion region. I_{tunn} describes the direct band-to-band tunnelling contribution, and I_X is the excess tunnelling current through defect states in the band gap.

The diffusion current of a magnetic pn-diode is given by

$$I_{diff} = Aqn_i^2 \left[\frac{D_{n\uparrow} e^{\Delta/2k_BT}}{2L_{n\uparrow} N_A} + \frac{D_{n\downarrow} e^{-\Delta/2k_BT}}{2L_{n\downarrow} N_A} + \frac{D_p}{L_p N_D} \right] \left(e^{q(V - R_S I_{tot})/k_BT} - 1 \right), \tag{6}$$

where A is the area of the diode, n_i is the intrinsic carrier concentration, $D_{n\sigma}$ (D_p) is the carrier diffusion coefficient for the electrons (holes), $L_{n\sigma}$ (L_p) is the diffusion length of the electrons (holes), and N_A(N_D) is the acceptor (donor) concentration. R_S is the series resistance of the diode.

The series resistance R_S in (6) depends on the magnetic ordering, if the spin disorder scattering dominates the charge transport in the magnetic layer. The model (6) predicts

large magnetoresistance, if the following conditions are fulfilled: the thermal energy must be smaller than the band splitting parameter, the diffusion current should dominate, and the acceptor doping should be larger than the donor doping, and ferromagnetism exists also in the depletion layer.

Also the tunnelling current in a pn-diode depends on the magnetic field, and the current is given by

$$I_{tunn} = AC\sum_{\sigma}\int_{E_c(n)}^{E_v(p)} T_{\sigma}(E)\left[f_C(E)-f_V^{\sigma}(E)\right]D_C(E)D_V^{\sigma}(E)dE \tag{7}$$

where C is a constant, and $E_c(n)$ and $E_v(p)$ are the band edges of the conduction band on the n-side and the valence band on the p-side, respectively. T_{σ}(E) is the spin-dependent tunnelling probability, $f_C(E)$ and $f_V^{\sigma}(E)$ are the Fermi-Dirac distribution functions, and $D_C(E)$ and $D_V(E)$ are the densities of state for the conduction and valence bands, respectively:

$$D_C(E) = \frac{M_C m_{de}^{3/2}\sqrt{2}}{\pi^2\hbar^3}(E-E_c)^{p_1} \tag{8}$$

$$D_V^{\sigma}(E) = \frac{1}{2}\frac{m_{dh}^{3/2}\sqrt{2}}{\pi^2\hbar^3}\left[E_v - E - \frac{\Delta}{2}\left(\delta_{\sigma\uparrow}-\delta_{\sigma\downarrow}\right)\right]^{p_2}, \tag{9}$$

where Δ is given by (2). The maximum relative current change $\Delta I_{tun}/I_{tun}$ can be estimated from (7) to (9) and it is about -5 % at B < 1T with the typical material parameters for Mn-doped GaAs [Publication IV]. The third component of the total current that may depend on the magnetic field is the temperature independent excess current. It is defined as

$$I_X = AI_V \exp\left[\frac{4}{3}\left(\frac{m_r^*\varepsilon_s}{N^*}\right)^{1/2}(V - R_s I_{tot} - V_V)\right], \tag{10}$$

where I_V is the current at a valley voltage V_V, and $N^* = N_A N_D/(N_A+N_D)$. The magnetic field dependence is a result of the MR of R_S. In Fig. 2 the I-V characteristics of a spin Esaki-Zener tunnel diode is presented with different band splitting parameters and different p- values (related to Eqs. (8) and (9)). It can be seen that in the case of a

parabolic band (*p=1/2*) the magnitude of the current depends strongly on the band splitting parameter. The shape of the valence band is also important, since in the case of *p=3/2* the magnetic field dependent current is typically larger than the non-magnetic current (Δ=0) and in the case of *p=1/2* it is typically vice versa.

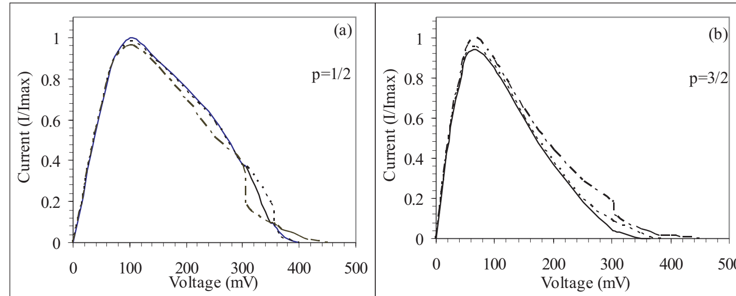

Fig.2. *Calculated I-V characteristics in a ferromagnetic spin Esaki-Zener tunnel diode in the case (a)* $p_2 = 1/2$*, and (b)* $p_2 = 3/2$*. The solid curves show the tunnelling currents when there is no band splitting,* $\Delta_2 = 0$*, and the dashed and dotted curves show the results in the cases* $\Delta = 0.1eV$ *and* $\Delta = 0.2eV$ *, respectively. Data taken from Publication I.*

3.2 Modeling of the Resonant Tunnelling Diode (RTD) with a Ferromagnetic Emitter

The resonant tunnelling diode was the first actual DMS spintronic device where band splitting was observed [55]. In the emitter of a RTD the valence band will split into two spin polarized subbands due to the giant Zeeman effect (see Eq. (1) and Fig 3.), when the magnetic field is applied, and it will change the tunnelling current.

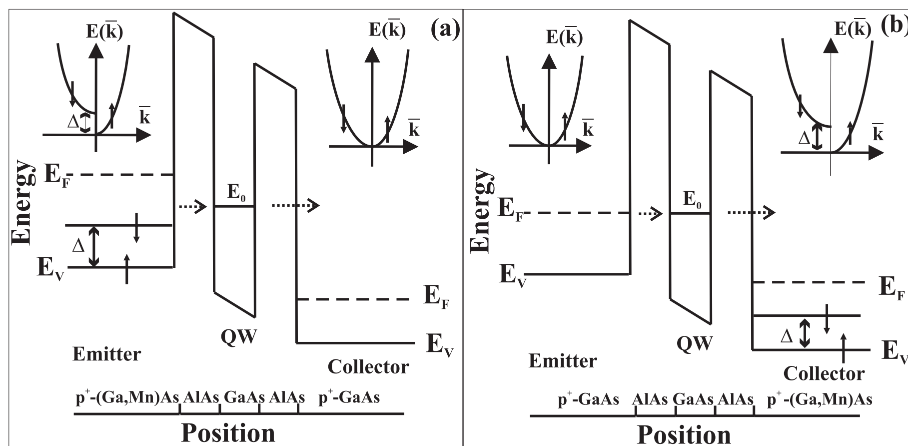

Fig 3. *Band diagram for a RTD with a ferromagnetic emitter, and (b) with a ferromagnetic collector, both in the case of a non-zero band splitting,* $\Delta > 0$.

The ordinary resonant tunnelling diode was invented by Tsu and Esaki [56] and they derived the well-known Tsu-Esaki formula for the current. When the band splitting is taken into account, the tunnelling current of a RTD with a ferromagnetic emitter is given by the modified Tsu-Esaki formula [57]

$$J_T = J_T^{\uparrow} + J_T^{\downarrow} = \int_0^{\infty} T_{\uparrow}(E) S_{\uparrow}(E)\, dE + \int_{\Delta}^{\infty} T_{\downarrow}(E) S_{\downarrow}(E)\, dE \qquad (11)$$

where $T_\sigma(E)$ is the quantum mechanical transmission coefficient through the double barrier structure given by the following Lorenzian:

$$T_\sigma(E) = \frac{\Gamma_L \Gamma_R}{(\Gamma/2)^2 + \left(E - E_\sigma^{res}\right)^2} \qquad (12)$$

Here $\Gamma = \Gamma_L + \Gamma_R$ is the spin-independent full width of the half-maximum of the resonance. The partial widths Γ_L and Γ_R for the left and right barriers, respectively, can be calculated in a straightforward manner in the case of the rectangular barriers [58]. In Eq.(11) we have taken the bottom of the spin-up subband as a zero level for the energy *E*. Then the energy of the resonant level E_σ^{res} in Eq.(12) is given by

$$E_\sigma^{res} = E_0 - \frac{qV_{QW}}{2} + \frac{\Delta}{2}\left(\delta_{\sigma\uparrow} - \delta_{\sigma\downarrow}\right) \qquad (13)$$

Here E_0 is the energy of the single quantized level in the quantum well, when there is no band splitting, i.e., when $\Delta = 0$. The voltage V_{QW} over the double barrier structure is assumed to be divided equally between the two barriers. The supply function $S_\sigma(E)$ in Eq. (11) is given by

$$S_\sigma(E) = \left(\frac{qm^* k_B T}{4\pi^2 \hbar^3}\right) \ln\left[\frac{1 + e^{\left(E_{F\sigma}^L - E\right)/k_B T}}{1 + e^{\left(E_{F\sigma}^R - E\right)/k_B T}}\right] \qquad (14)$$

where $E_{F\sigma}^{L(R)}$ is the Fermi energy of the spin-polarized subband on the left (right) side, when the bottom of the spin-up band is chosen as the zero level for the charge carrier energy:

$$E_{F\sigma}^{L,R} = E_{F0}^{L,R} + \frac{\Delta}{2}\left(\delta_{\sigma\uparrow} - \delta_{\sigma\downarrow}\right) \tag{15}$$

and $E_{F0}^{L} = \hbar^2\left(3\pi^2 p\right)^{2/3}/2m*$ is the quasi-Fermi level of the holes before the band splitting, $E_{F0}^{R} = E_{F0}^{L} - qV_{QW}$, and p is the hole concentration. The expression (Eq.(11)) reduces to the well-known Tsu-Esaki formula in the case of no band splitting, i.e., when $\Delta = 0$. The graphs in Fig. 4 have been calculated from Equation (11). It can be seen that the resonant peaks will split into two when the magnetic field is applied. This behaviour has been experimentally seen by Ohno [55].

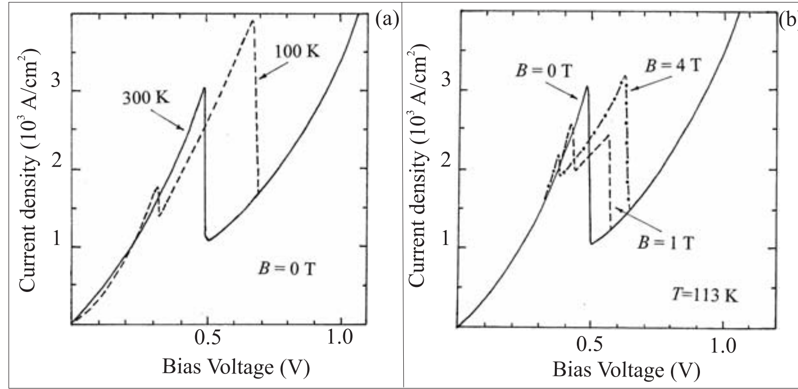

Fig.4.(a) *Calculated I-V characteristics for a magnetic RTD with an emitter made of Mn-doped GaAs, when there is no external magnetic field.* **(b)** *Calculated effect of the external magnetic field on the I-V characteristics of a magnetic RTD at 113 K, when T_C = 110 K. Data taken from Publication V.*

4. Experimental Techniques and Fabrication of the Magnetic Thin Films and Diodes

The biggest problem in the fabrication of the DMS thin films is the segregation of magnetic atoms during the growth process. The problem was solved when Munekata et. al. [10] realized that by decreasing the growth temperature inside the MBE chamber the segregation problem could be avoided. The temperature region is very limited in the growth process. In Fig. 5 the relation between the growth temperatures, Mn doping and the properties of the thin film are shown.

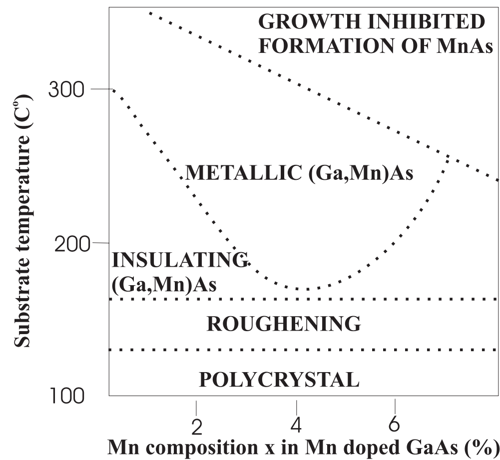

Fig. 5. *Substrate temperature and Mn composition. Data taken from [14].*

4.1 Molecular Beam Epitaxy

The Molecular Beam Epitaxy (MBE) technique was developed by J.R Arthur [59] and A.Y. Cho [60] in the late 1960's and the early 1970's. The MBE growth technique is based on thermal molecular beams, which can be controlled very accurately. The growth process takes place under ultrahigh vacuum (UHV) conditions. The MBE method has many advantages and therefore it is the most popular growth method for DMS thin films and DMS devices. Firstly, due to slow growth rate and epitaxial growth the interface between different materials can be of high quality and sharp. Secondly, also the doping profiles can be very sharp. Thirdly, the variety of semiconductors that can be grown and dopants used in MBE are very large. Also the problems related to contamination are reduced due to the fact that the growth is done in UHV.

A disadvantage of the MBE method is that the growth rate is very slow (typically 1μm/hour) [61].

In the MBE growth the materials are in separate effusion ovens. Every oven has a shutter of its own and a temperature control. The temperature control determines the intensity of the thermal molecular beam and the shutter controls the time interval during which the thermal molecular beam hits the sample. Additionally, the pressure of the oven has an effect on the growth process. The substrate is also heated, but the temperature is much lower compared to the ovens. The temperature of the substrate defines the growth mode, composition of the thin film and the growth rate. The substrate holder is continuously rotating in order to gain a uniform layer [61]. Other factors affecting the growth are the surface reactions, substrate film reactions, evaporating sources and geometry [61]. The schematic figure of the VG100H MBE system used in the Electron Physics Group in the Micro and Nanosciences Laboratory is illustrated in Fig. 6.

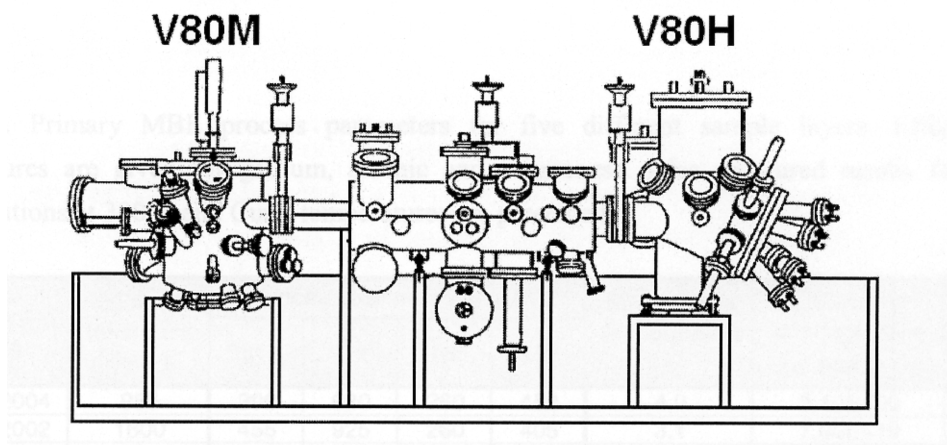

Fig.6. *Schematic picture of a MBE system [61]*

4.2 Fabrication of Mn Doped GaAs Thin Films and Diodes

4.2.1 Mn doped GaAs Thin Films

The Mn doped GaAs thin films were fabricated in our VG100H MBE system. All our thin films were grown on semi-insulating GaAs (100) substrates. First, the surface was cleaned and possible oxide removed. After that a buffer zone of 50 nm undoped GaAs was grown at 580 ^{o}C. Then the growth temperature was decreased to 230 ^{o}C and a 1 μm thick Mn doped GaAs layer was grown. The Mn content was changed between 1% and 9 %, but only the samples in which the concentration was 3%-5% exhibited ferromagnetism. During the growth process the crystal quality was examined by Reflection High Energy Diffraction. Finally the ohmic Pt/Ni/Pt/Au contacts to the p^{+}-layer were made using an e-beam vacuum evaporation technique. A more detailed description can be found in Publication III.

4.2.2 Mn Doped GaAs Pn-diodes

After the fabrication process of Mn doped GaAs thin films were under control, we started to fabricate pn-diodes. The structure of the diode is shown in Fig. 7. The doping concentration of the n-type GaAs substrate was 10^{17} cm^{-3}. On top of the substrate a 250nm thick n+ doped GaAs thin film was grown. The doping concentration of the n+ layer was either 10^{17} cm^{-3} (normal pn-diodes) or 10^{19}cm^{-3} (spin Esaki-Zener tunnel diodes). Above the n^{+}-layer there is a 0.5 μm thick Mn-doped p^{+}-layer. The growth procedure of that layer was the same as that described in Chapter 4.2.1. Pt/Ni/Pt/Au and Au/Ge/Ni/Au contacts were evaporated on the front side and back sides, respectively.

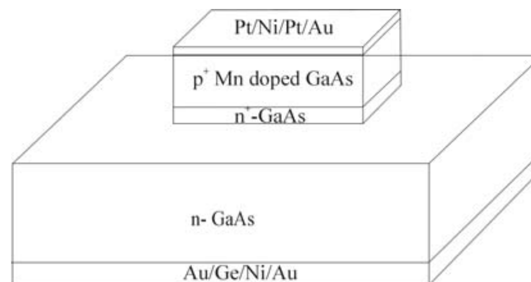

Fig.7. *Schematic structure of the magnetic p-(Ga,Mn)As/n-GaAs-diode.*

4.2.3 Magnetic RTD with Magnetic Emitter

The magnetic RTDs were grown using both molecular beam epitaxy (MBE) and metal-organic vapor phase epitaxy (MOVPE) growth techniques. The substrate was heavily p-doped and the carrier concentration was $p = 1.3 \cdot 10^{19} cm^{-3}$. After that a 100 nm p-type GaAs buffer layer ($p = 3 \cdot 10^{19} cm^{-3}$) was grown using MOVPE. Next the quantum well structure was grown by MOVPE. The structure consisted of several 5nm or 7nm undoped GaAs and AlAs barriers (Fig. 8). Finally, a 500 nm thick Mn-doped magnetic GaAs layer was grown using MBE at a low temperatures (T=230 ^{0}C). The front side contact was made using a lift off process and the metallization consisting of 5/10/100 nm thick Au/Ti/Au was evaporated. After that the final structure was obtained by mesa etching. The backside contact of 5/10/100 nm thick Au/Ti/Au was evaporated. Then a 50 μm thick copper layer was electroplated on top of the Au/Ti/Au contacts. Finally, using indium the RTD was soldered to a polyimide sample holder, and Al wires with a diameter of 100 μm were bonded to the contact pads. A more detailed description can be found in Publication V.

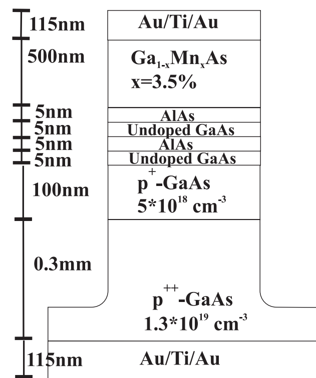

Fig.8. *Schematic structure of the fabricated magnetic RTD.*

4.3 Mn Doped GaN Thin Films and Pn-diode

4.3.1 Mn Doped GaN Thin Films

On top of the sapphire (0001) substrate a 2 μm thick undoped GaN layer was grown by MOVPE. After that the fabrication process continued with a deposition of a 50nm thick Mn layer on top of the sample using the MBE system. Then the Mn diffusion was

activated by annealing the samples under UHV conditions for 14 hours at 600°C. The excess Mn layer was removed from the GaN surface by dipping the samples in HCl for a couple of seconds. The ohmic contacts to the samples were made using copper (98%)/beryllium (2%) wires. The sample sizes were 64 mm^2.

The fabrication process is very difficult and therefore not very repeatable. Often the samples were inhomogeneous, causing problems for electrical measurements. Some of the samples were also destroyed in the HCl dipping phase.

4.3.2 Mn Doped GaN Pn-Diode

The fabrication of the (Ga,Mn)N pn-diodes was started by growing a p-type layer of GaN on top of the sapphire substrate. The growth was made by MOVPE. In order to fabricate a pn-junction some part of the p-type GaN was changed to n-type by Mn doping. The fabrication process of the n-side is similar to the one in Mn doped GaN thin films, i.e., solid state diffusion is utilized. The metallization of the diode was made using an e-beam evaporator.

5. Results

5.1 Magnetic Mn Doped GaAs Thin Films

The Mn doped GaAs thin films were first characterized by measuring the resistivity as a function of temperature (Fig. 9 (a)) [Publication IV]. The behavior of the resistivity curves changed from insulating to metallic, when the hole concentration of the thin film increased. In Fig. 9 (a) the solid lines have been calculated using the the Dubson-Holcomb (DH) model [62]. Together with the model for spin disorder scattering, the resistivity in the DH-model is given by

$$\rho_{DH}(T) = \rho_{300K}\left(\frac{300K}{T}\right) / \ln\left[1 + \exp\left(\frac{E_m - E_F}{k_B T}\right)\right], \tag{20}$$

where E_m is the mobility edge in a disordered semiconductor The model parameters can be found in Table 1. The only truly varying parameter is the E_m-E_F , which varies from -0.2 meV (uppermost curve of Fig. 9 (a)) to 6.5 meV (the lowest curve in Fig. 9 (a)) [Publication IV].

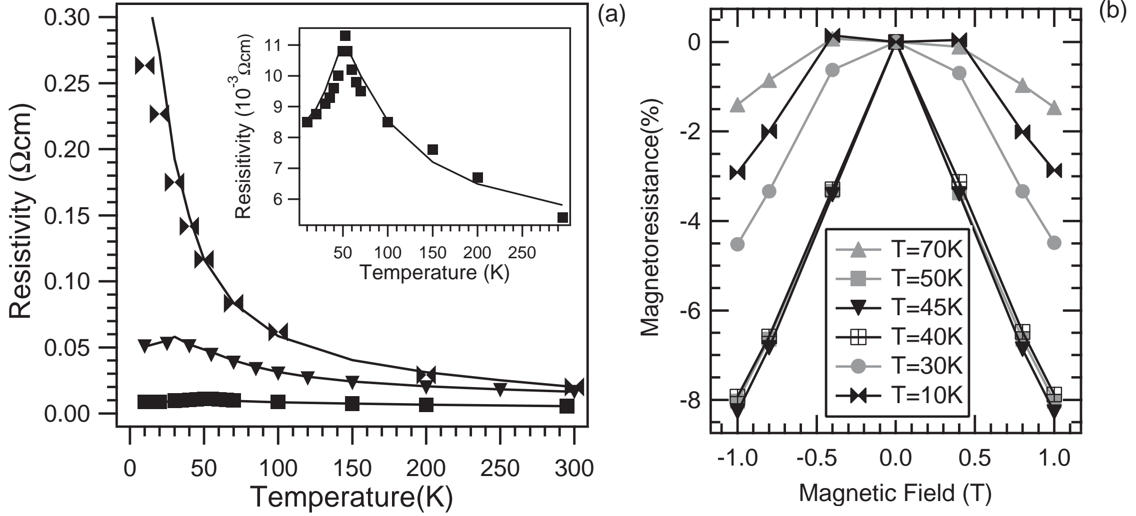

Fig.9. **(a)** *Resistivity vs. temperature in $Ga_{1-x}Mn_xAs$ layers with the room temperature hole concentrations* $5.6 \cdot 10^{19}\,cm^{-3}$, $7.0 \cdot 10^{19}\,cm^{-3}$ *, and* $1.7 \cdot 10^{20}\,cm^{-3}$ *(from top to the bottom). The solid curves have been calculated by combining the spin disorder scattering model with a Dubson-Holcomb-model [62] for disordered semiconductors near the metal-semiconductor transition. The inset shows the lowest curve in more detail.* **(b)** *Magnetoresistance* $\left[\rho(B) - \rho(0)\right] / \rho(0)$ *vs. magnetic field at various temperatures in $Ga_{1-x}Mn_xAs$ with x=0.04 (*$7.0 \cdot 10^{19}\,cm^{-3}$*). Data taken from Publication IV.*

In order to study the ferromagnetic properties of Mn doped GaAs thin films, the magnetoresistance as a function of magnetic field at various temperatures was also measured (Fig. 9(b)). The negative magnetoresistance of the samples is a clear indication of spin-disorder scattering. The Curie temperature can be estimated to be about 45 Kelvin, since the magnetoresistance has its maximum at that temperature.

Table 1. *Parameters of Mn doped GaAs used in the graph in Fig 9. (a)[Publication IV]*

Exchange coupling parameter	J_{exch}	2.4 eV
Lattice constant	a_0	5.65 Å
Effective mass	m^*	0.5 m0
Curie temperature	T_C	30 K

In addition, the Hall resistivity measurement results proved that the samples were ferromagnetic, since the relation between the Hall resistivity and magnetic field was not linear below 50 K [Publication IV]. Finally, the ferromagnetism of the samples was verified by a direct magnetization measurements (Fig.10). The measurements confirmed that the Curie-temperatures of the samples were between 30-60 K.

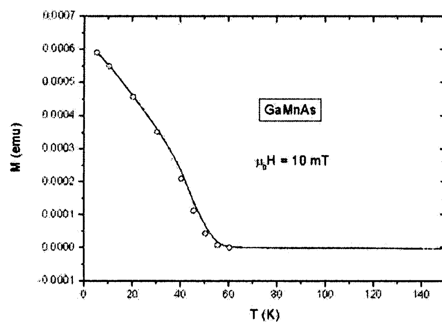

Fig. 10. *Magnetization measurement of Mn doped GaAs thin film.*

5.2 Magnetic Mn Doped GaAs Pn-diodes

After the discovery of ferromagnetism in Mn doped InAs and GaAs many groups have developed theories of DMS pn-diodes [63-64] and [54]. In most of the fabricated magnetic pn-diodes both sides are heavily doped, so the diodes operate in the tunnelling

region. Those diodes are called tunnel-diodes or Zener-diode or Esaki-diode or spin Esaki-Zener tunnel diode.

The tunnel-diodes have also been used to study the spin polarization and spin tunnelling properties in DMS. Kohda et. al. [65] and E. Johnston-Halperin et. al. [66] fabricated a tunnel diode and an LED structure and demonstrated the spin injection of the electrons between the ferromagnetic and the nonmagnetic layer. Dorpe et. al. [67] improved the same structure by fabricating an AlGaAs layer in addition to a GaAs layer. Their LED structure showed 60% spin polarization.

The spin Esaki-Zener tunnel-diodes operate in a tunnelling mode and therefore they can be used to study the spin-dependent tunnelling. The new observed phenomena related to Mn doped GaAs is the TAMR effect in tunnel diode structure. The TAMR effect in a p^+-(Ga_{1-x},Mn_x)As/n^+-GaAs Spin Esaki-Zener tunnel was observed for the first time independently by both Holmberg et. al. [Publication I] and Giraud et. al. [50]. The same effect was also later observed by Ciorga et. al. [68].

An excellent theoretical paper of TAMR in p^+-(Ga,Mn)As/n^+-GaAs spin Esaki-Zener tunnel diode was given by Sankiwski et. al. [49] ,e.g., they calculated that TAMR should decrease if the hole concentration increases on the magnetic side and increase if the nonmagnetic n-type layer is more heavily doped. In the same article also TMR of trilayers p-(Ga_{1-x},Mn_x)As/GaAs/ p-(Ga_{1-x},Mn_x)As is shown to be dependent on the band offset. The TMR ratio increases, when the nonmagnetic layer is replaced by AlAs, since the band offset is larger. Also the TMR is larger, if the tunnel barrier is thinner and higher.

In our studies two different magnetic (Ga,Mn)As/GaAs pn-diodes were fabricated having either lightly (normal pn-diodes) or a heavily doped (spin Esaki-Zener tunnel diodes) non-magnetic n-type layer. When the non-magnetic n-side was lightly doped, no magnetic field dependence of the *I-V* curve was observed. There are several possible reasons for that [Publication IV]

(A) If the magnetic p-side is more heavily doped than the non-magnetic n-side, then the current in the non-magnetic side of the diode may dominate and therefore the current does not depend on the band splitting parameter Δ (Fig. 11 (a)).

(B) The band splitting parameter Δ may be much smaller than the thermal energy even at low temperatures

(C) The band discontinuity between the n-GaAs and p-(Ga,Mn)As may cause the current to flow via a thermionic emission over the barrier (Fig. 11 (b)).

(D) The absence of free carriers in the depletion layer causes no ferromagnetism ordering to occur, since the ferromagnetism in Mn doped GaAs is hole mediated (Fig. 11. c)

(E) The excess current (10), which does not depend on the magnetic field dominates at low temperatures (lower than T_C)

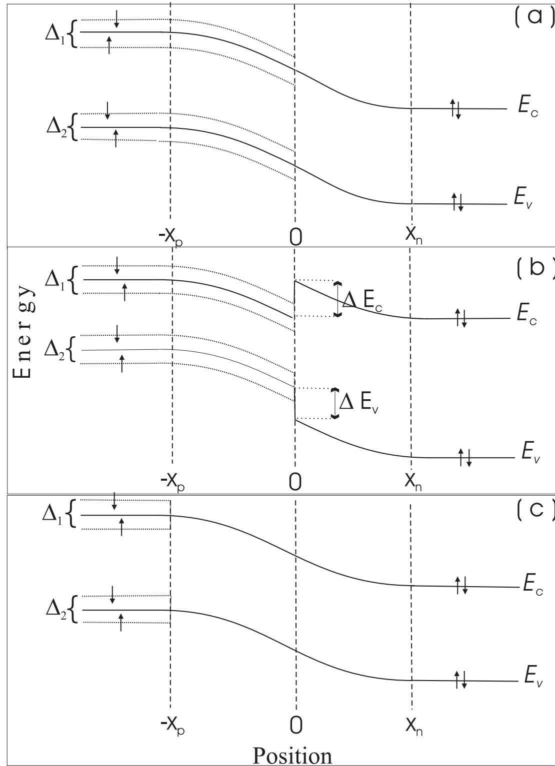

Fig.11. *Schematic energy band diagrams vs. position for a magnetic pn-diode, where the p-side is ferromagnetic and the n-side non-magnetic. The dashed curves show the spin-polarized sub-bands. (a) Magnetic ordering extends to the depletion region on the p-side ($-x_p \le x \le 0$). (b) Band discontinuities ΔE_c and ΔE_v are included at $x = 0$. (c) The whole depletion region, including the p-side, is non-magnetic in the case of carrier-induced ferromagnetism. $\Delta_1 = xJ^{sd}_{exch}\langle S^z \rangle$ and $\Delta_2 = xJ^{pd}_{exch}\langle S^z \rangle$ are the band splitting parameters for the conduction and valence bands, respectively.*

Explanation (A) can be ruled out, since even in the case when the doping concentrations were about same, no magnetic field dependence was observed at higher biases, where the diffusion current dominates in ordinary pn-diodes. The alternatives (B) and (C) cannot explain the phenomenon, since the band splitting parameter Δ is much larger in Mn doped GaAs (about 0.2 eV) than the thermal energy at low temperatures and ΔE_C is also quite small [Publication IV]. In the depletion layer there are really few free holes and therefore there might not be enough free holes to mediate the ferromagnetism. The measured *I-V* curve [Publication IV] also has a very weak temperature dependence and the excess current is the only component of the current which has a very low temperature dependence. As mentioned earlier, the excess current does not depend on the magnetic field. We can conclude that explanations (D) and (E) are the possible reasons for the absence of magnetoresistance in the Mn- doped GaAs pn-diodes but based on the obtained data we cannot determine which one dominates.

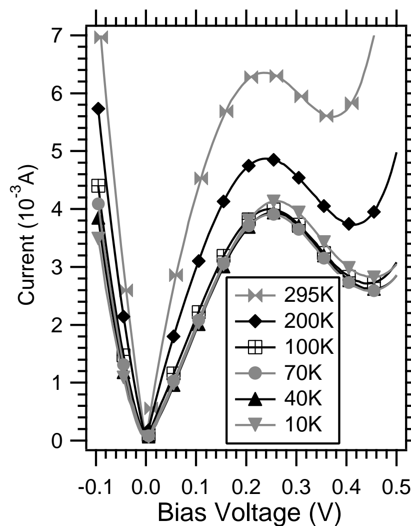

Fig.12. *Measured I-V characteristics at various temperatures in a ferromagnetic (Ga,Mn)As/GaAs tunnel diode (B=0T). Data taken from Publication III.*

When also the non-magnetic side was heavily doped, we got a magnetic (Ga,Mn)As/GaAs-$p^{++}n^{++}$ spin Esaki-Zener tunnel diode. The magnetization of the sample was verified by a direct magnetization measurement. In Fig. 12. the *I-V* characteristics of a magnetic tunnel diode as function of temperature is presented. The temperature dependence of the *I-V* curve becomes weaker when the temperature decreases. This is due to the fact that at low temperature the *T*-independent tunnelling

current (7) and excess current (10) are larger than the T-dependent recombination current and diffusion current (6).

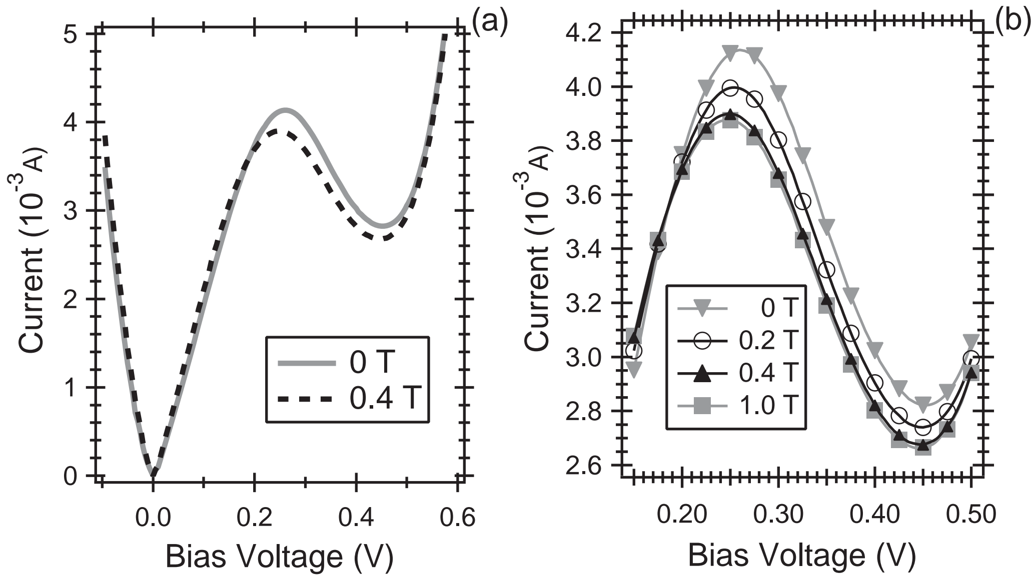

Fig.13. (a) *Measured I-V characteristics in a (Ga,Mn)As/GaAs tunnel diode at T= 10 K with and without magnetic field* **(b)** *Measured I-V characteristics in the voltage region where the tunnelling current dominates in various magnetic fields. Data taken from Publication IV.*

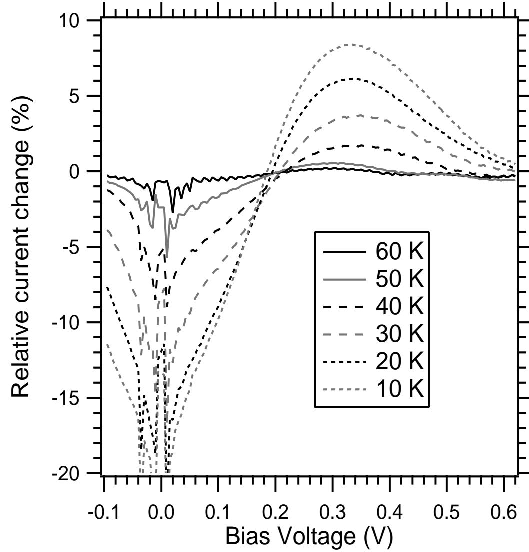

Fig. 14. *The relative current* $(I(B)-I(0))/I(0)$ *change is presented as function of bias voltages at various temperatures. Data taken from Publication I and IV.*

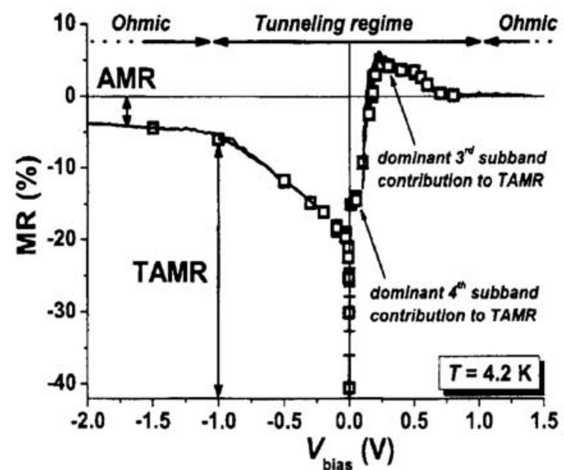

Fig. 15. *Magnetoresistance of (Ga,Mn)As/GaAs tunnel diode as a function of bias voltage. Figure taken from Ref. [50]*

As seen in Fig. 13. the *I-V* characteristics of a tunnel diode has a magnetic field dependence at low temperatures. A large positive magnetoresistance was observed both at low reverse and positive bias voltages (Fig. 14). At higher positive bias voltages the magnetoresistance was positive and at smaller positive and negative bias voltages the magnetoresistance was negative. The observed behavior can be explained well by the tunnelling anisotropic magnetoresistance (TAMR) effect. In our study a very large magnetoresistance at low bias voltages about 20% at 10 K was observed. Our result is in good agreement with Giraud et. al. [50], since they observed 40 % magnetoresistance at 4.2 K (Fig. 15). In addition, the magnetoresistance saturates under high magnetic fields (Fig. 16). The theoretical explanation to the TAMR effect is given in Chapter 2.4.

This effect could be used in ultra-low power spintronic devices, since the magnetoresistance changes rapidly by a small increase of the bias voltage. TAMR can also be used in the spectroscopy and the valence band structure studies in Mn doped GaAs [Publication I]. An excellent example of the capability of the spectroscopy can be seen in Fig. 15 [50], where even the 3rd and 4th subbands can be seen.

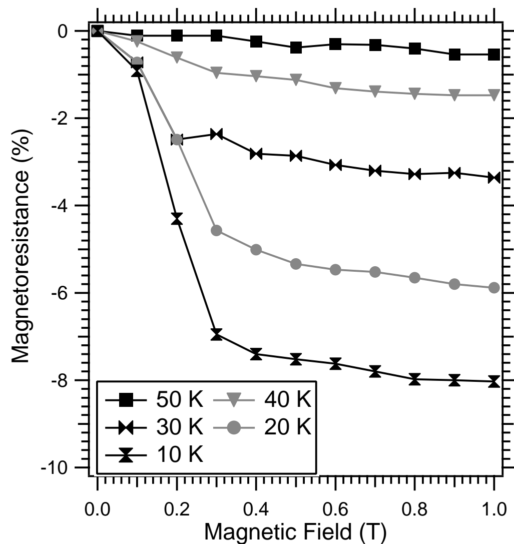

Fig.16. *Relative change of the tunnelling current* $(I(B)-I(0))/I(0)$ *vs. magnetic field at various temperatures in a (Ga,Mn)As/GaAs tunnel diode at V=300 mV. Data taken from Publication IV.*

5.3 Magnetic RTD with Magnetic Emitter

The research of RTD has been intensive for many decades. The effect of a magnetic field on the *I-V* characteristics of nonmagnetic GaAs/AlAs RTD was for the first time studied by Mendez [69] and Hayden [70]. It was observed that high parallel [69] and perpendicular [70] magnetic fields (B>2T) change the *I-V* characteristics of RTD. After the discovery of the DMS materials, the magnetic field dependence of the paramagnetic ErAs quantum well in the GaAs based AlAs/ErAs/AlAs structure was studied by Bremer et. al. [71]. A large spin splitting of the electronic states in the quantum well under high magnetic fields was observed. The first actual ferromagnetic quantum well in a RTD structure was fabricated by Haury et. al. [72]. Their group used CdMnTe technology, but the Curie-temperature was very low, about 2K.

The next major development step was achieved when Ohno et. al. [55] and [73] were able to fabricate a RTD structure with a ferromagnetic Mn doped GaAs emitter. A large spontaneous spin-splitting of the valence band in the ferromagnetic emitter was observed in the *I-V* characteristics. The band splitting was observed without applied magnetic field in two peaks LH1 and HH2 when the temperature was below 80 K (T_C was about 70 K). They also noticed that the Mn doped GaAs emitter causes the shift of peaks as a function of the magnetic field [73]. Also Ohya et. al. [74] studied the same structures as Ohno, except that the quantum well was also ferromagnetic. The results were slightly different than those observed by Ohno et. al. [55], since no resonance peaks at positive bias were observed. They suggested that it might be due to the Fermi energy difference between the magnetic emitter and the non-magnetic collector. The measured tunnelling magnetoresistance was over 10 % at 2.6 K.

In our studies the *I-V* characteristics of non-magnetic GaAs RTDs were measured first to check how large the magnetic resistance is in a non-magnetic RTD (Fig. 17). In the non-magnetic RTD three resonant peaks both at negative and positive bias were observed. The magnetic field dependence of the current was relative small (<0.3 %) as seen in the inset of Fig. 17.

Next the fabricated structures of RTDs were the same except that the emitter was doped with Mn. The RTDs with a magnetic emitter can be divided into two categories depending on the doping level. When the Mn doping level of the emitter is below 4 %, the emitter is semiconducting and if it is above 4 %, the emitter is metallic.

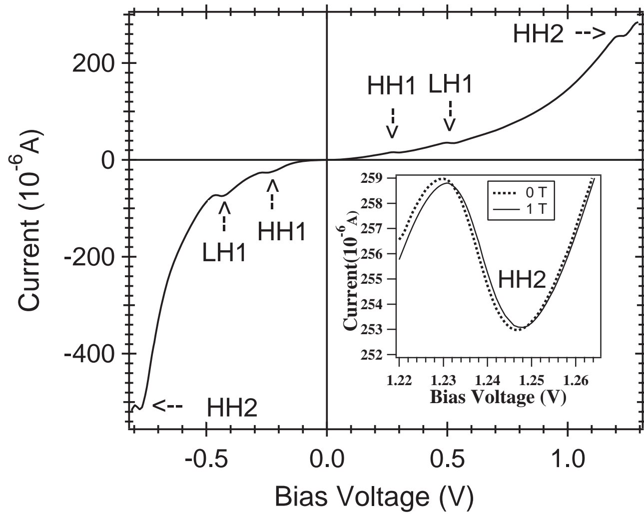

Fig. 17 *I-V characteristics of a non-magnetic GaAs RTD at 8 K. The inset shows the effect of the magnetic field on the HH2-resonant peak. Data taken from Publication V.*

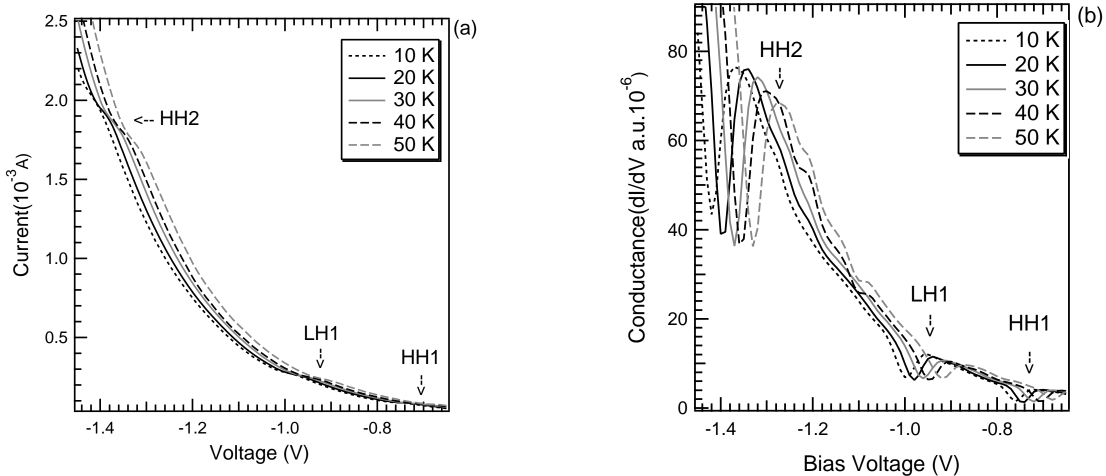

Fig.18. **(a)** *I-V characteristics of a magnetic RTD with a metallic (Ga,Mn)As emitter at various temperatures.* **(b)** *Conductance dI/dV vs. negative bias voltage at various temperatures. In both figures the external magnetic field was zero. Data taken from Publication V.*

The *I-V* characteristics and conductance *dV/dI* at various temperatures in the case of a metallic emitter RTD are shown in Fig. 18. At negative bias voltage the three resonant peaks HH1, LH1 and HH2 were seen. However, no resonant peaks were seen at positive bias voltages and this is probably due to the large Fermi-energy in the heavily doped

emitter. The magnetic field dependence was largest in the HH2 peek and its *I-V* characteristic is shown in Fig. 19. (a). As shown in Fig 19. (b) the magnetoresistance will saturate as the applied magnetic field increases. The behavior can be explained by the TAMR effect and to the best of our knowledge; this is first time TAMR has been observed in a RTD structure [Publication V].

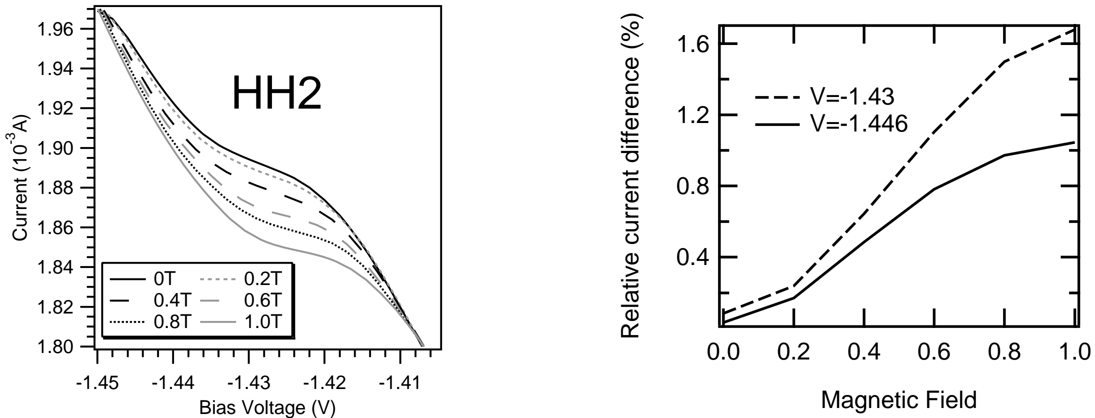

Fig.19. (a) *I-V characteristics of the magnetic RTD with a metallic emitter in various magnetic fields at T = 8 K for negative bias voltages around the resonance peak HH2.* **(b)** *Magnetic field dependence of the tunnelling current at the peak HH2 for two bias voltage values at T=8K. Data taken from Publication V.*

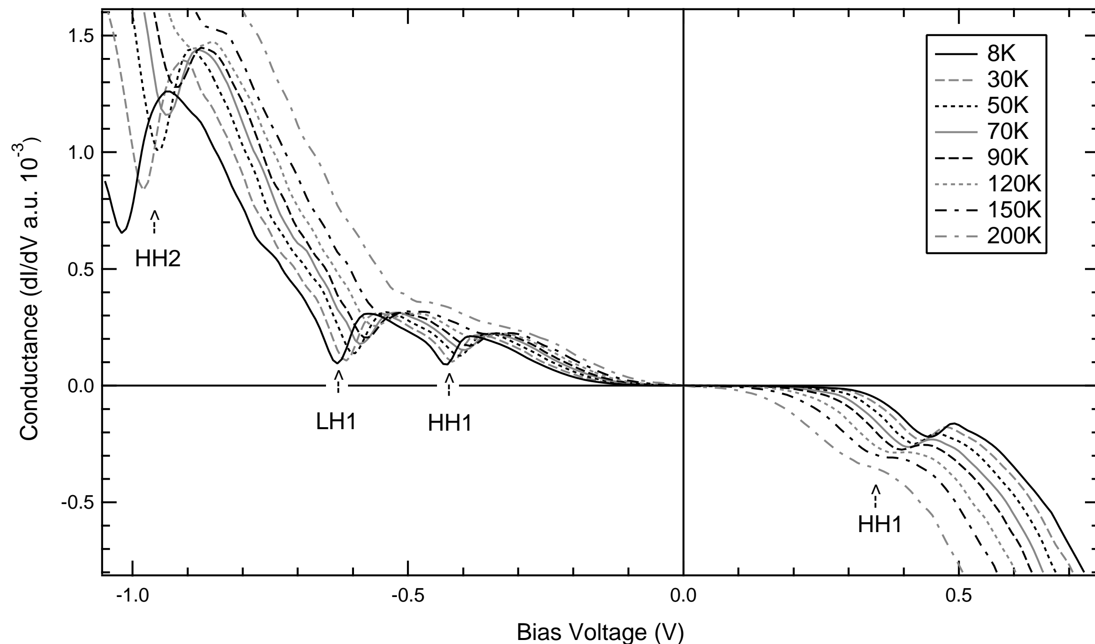

Fig. 20. *Conductance dI/dV vs. bias voltage at various temperatures in the magnetic RTD with a semiconducting emitter (B=0T). Data taken from Publication V.*

We also fabricated magnetic RTDs with a semiconducting emitter. The temperature dependence of the conductance is shown in Fig. 20. For the negative bias voltages the same three resonant peaks are observed as in a RTD with a metallic emitter, but in the positive region also one resonant peak was observed. It is due to smaller Fermi-energy for the holes in the case of the semiconducting emitter compared to the metallic emitter. Also the peaks are shown more clearly in the case of the semiconducting emitter.

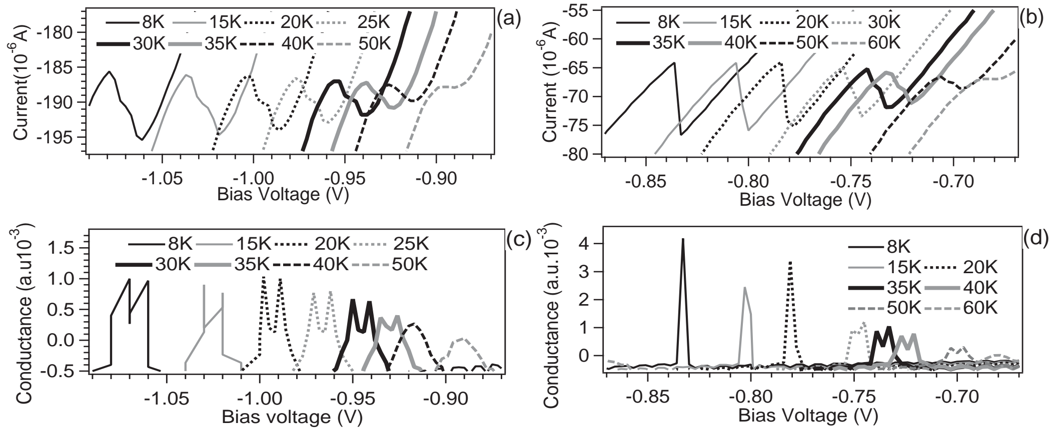

Fig. 21. *I-V characteristics of a FRTD with a semiconducting (Ga,Mn)As emitter at various temperatures for the first two peaks* ((**a**) *and* (**b**)). *Conductance dI/dV vs. negative bias voltage at various temperatures for the first two peaks* ((**c**) *and* (**d**))(*B= 0T in all cases*)

When the peaks were studied more carefully, it was found that the form of the peaks changed even without a magnetic field when the temperature was changed. The same double peak structures seen in Fig. 21. (b) have also been reported by Ohno et. al. [55] 1998]. Ohno's group stated that the double peak structure is caused by a valence band splitting due to the spontaneous magnetic ordering. However, we also observed the double peak structure in our magnetic RTDs, but we do not believe that it was caused by band splitting. Firstly, if the effect would be caused by the valence band splitting, the peak splitting should occur at the same temperature for both peaks, which is not the case as seen in Figs. 21 (c) and 21 (d). Secondly, the observed voltage difference between the double peaks does not depend on temperature or the magnetic field as it should be according to the model presented in ref. [75]. Finally, the kink seen in the *I-V* curve (Fig. 21(a)) has also been observed in non-magnetic RTDs [76]. It is due to the instability of a bias circuit caused by the negative differential resistance [76].

Next the magnetic field was applied and it was observed that the current is magnetic field dependent. However, the magnetic field dependence can be seen more clearly in the conductance curves (In Fig. 22). In the case of the semiconducting Mn-doped emitter the observed magnetoresistance could be explained by the negative magnetoresistance of the emitter layer, i.e., it is the series resistance effect.

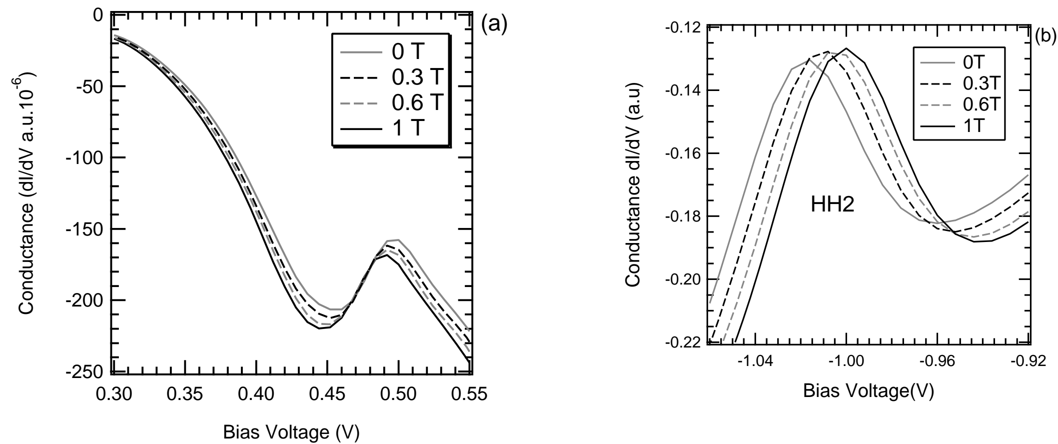

Fig.22. *Conductance dI/dV vs. bias voltage at T=8K in various magnetic fields* **(a)** *for the peak LH1 at positive bias voltages, and* **(b)** *for the peak HH2 at negative bias voltages. Data taken from Publication V.*

5.4 Results of Mn doped GaN Layers and Pn-diodes

The driving force in the research of the Mn doped GaN is the prediction made by Dietl [19] that Mn doped GaN exhibits ferromagnetism even at room temperature. In fact, many groups have observed this behavior (Table 2). However, there is a debate on what is causing the ferromagnetism. The problem is that the growth process of Mn doped GaN is very difficult and many other ferromagnetic compounds than (Ga,Mn)N can also appear as shown in Table 3. Additionally, it is difficult to heavily dope GaN in such a way that the diode would operate in the tunnelling mode. However, the advantage of Mn doped GaN is its high Curie temperature and that a lot of effort has been put into improving the GaN fabrication technology, since GaN is an important material for optoelectronics. Also the spin lifetime is about 20ns (5 K) even when the densities of charged dislocation are about $5*10^{18}$ cm^{-2} [87]. If the dislocation densities can be

reduced the spin lifetimes could be long also at room temperature. All of these good qualities of Mn doped GaN will make it possible to fabricate semiconductor spintronic devices, which operate at room temperature.

Table 2. *Curie-temperatures of fabricated (Ga,Mn)N thin films*

Reference	Tc	Mn%	Fabrication method
[77]	250 K	3	Nebulized spray pyrolysis
[78]	270 K	7,4	Implantation+MOVPE
[79]	550 K-700 K	0,06-0,5	Plasma-enhanced MBE
[80]	310-400 K	1	MOVPE
[81]	10 K-25 K	7	MBE
[20]	228 K-370 K	?	solid state diffusion
[22]	940 K	6 and 9	MBE
[82]	320 K (3 %)	3-12 %	MBE
[83]	550-700 K	0,0006-0,005	plasma-enhanced MBE
[84]	350 K	0,2-0,6	plasma-enhanced MBE

Table 3. *Different Mn compounds with their Curie-temperatures.*

Compound	T_C
Mn_2Ga [85]	690 K
Mn_3Ga [85]	743 K
Mn_5Ga_8 [85]	210 K
MnGa [85]	>300 K
Mn_4N [86]	738 K
Mn_3GaN [85]	200 K
MnN* [86]	650 K
Mn_3N_2* [86]	925 K
*Neels temperature	

They are only a few spintronic devices [88-90] fabricated from Mn doped GaN, since there are still problems in making good quality Mn doped GaN thin films. Buayanova et. al. [88] were able to fabricate a GaMnN/InGaN LED. They observed spin-polarization in this structure, but the problem was that they were not able to measure the photoluminescence spectrum at room temperature. The next major progress was made by Ham et. al. [89]. They fabricated ferromagnetic (Ga,Mn)N light-emitting diodes with an InGaN/GaN magnetic quantum well by MOVPE and plasma enhanced MBE. They manage to fabricate a Mn doped GaN layer with good quality and the electrical

properties of the diodes were really good e.g. the leakage current was 10 nA. They were able to observe the spin-polarization in the electromagnetic spectrum even at room temperature under a magnetic field. The observation was possible due to the better crystal quality and lighter doping of (In,Ga)N than in the previous studies [88], which led to a lifetime of spin high enough to be observed experimentally.

Reed at. al. [90] fabricated a Mn doped GaN p-i-n diode. The ferromagnetism was confirmed by direct magnetization measurement. However, in that article the magnetic field dependence on *I-V* characteristics was not measured. There have been also interesting proposals for new GaMnN based devices. One of the most interesting proposals was made by Li et. al. [91]. They proposed a magnetic GaMnN based resonance tunnelling diode, where the spin polarization could be controlled by an applied voltage without the external magnetic field.

In our studies [Publication II] we carried out the material characterization of the Mn doped GaN thin films in order to ensure that our growth method was functioning correctly. We used the solid state diffusion method to fabricate the Mn doped GaN and therefore it was important that the thickness of the actual magnetic layer was measured. The thickness of the Mn doped GaN layer was defined by Secondary Ion Mass Spectrometry (SIMS). The thickness of the Mn doped GaN was approximately 200-300nm. The samples were always n-type. The electron concentration was estimated to be about 10^{20} cm^{-3} and it was obtained using Hall and SIMS measurements. The value could not be defined more accurately since the maximum applied magnetic field of our magnet is only 1.3 T and in the SIMS measurement there was no Mn reference. In addition, the crystallographic structure was measured using the X-ray Diffraction (XRD) method. XRD and SIMS results indicated that some segregation of Ga_xMn_y in (Ga,Mn)N is present in our samples.

Also the Hall resistance (Fig. 23.) and magnetoresistance (Fig. 24.) as function of magnetic field were measured in order to study the magnetotrasport properties of Mn doped GaN thin films and prove that our samples are ferromagnetic above room

temperature. The Curie temperature of the Mn doped GaN thin films can be estimated to be about 330 K according to the Hall resistance measurement results. In addition, the largest measured magnetoresistance 1.3 % was observed at 330 K, which confirms that the Curie-temperature is about 330 K. Finally, the Curie temperature was verified by a direct magnetization measurement (Fig. 25).

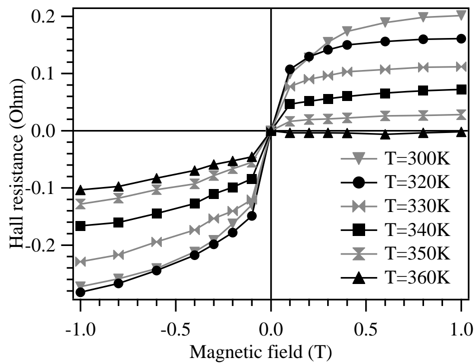

Fig. 23. *Hall resistance versus magnetic field at various temperatures in (Ga,Mn)N. Data taken from Publication II.*

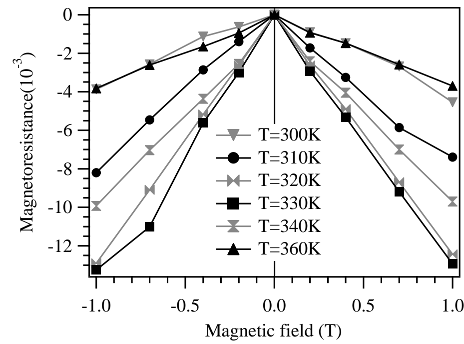

Fig. 24. *Magnetoresistance versus magnetic field at various temperatures in (Ga,Mn)N. Data taken from Publication II.*

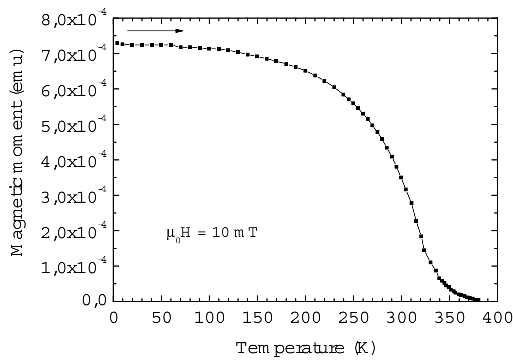

Fig. 25. *The magnetic moment of Mn doped GaN thin film as a function of temperature. Data taken from Publication II.*

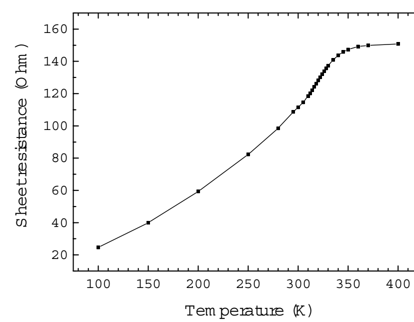

Fig. 26. *Sheet resistance as a function of temperature in (Ga,Mn)N. Data taken from Publication II.*

The measured sheet resistance as a function temperature is shown in Fig. 26. The behavior can be explained by spin-disorder scattering (1) via metals [92], which can be described by the following formula for resistivity

$$\rho_s(T,B) = \rho_0\left[S(S+1) - \left\langle \vec{S}(T,B)\right\rangle^2\right]. \tag{20}$$

At temperatures higher than the Curie temperature the resistivity is constant, since $\langle \vec{S} \rangle$ =0. Below the Curie temperature the resistivity starts to decrease, since below T_C $\langle \vec{S} \rangle$ starts to increase. As seen in Fig. 26 the constant behavior starts at about 330 K and as mentioned earlier that is the Curie temperature of our sample.

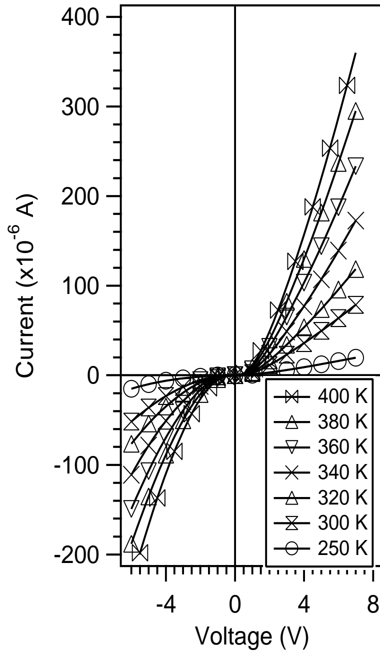

Fig. 27. *Current in GaN:Mn/GaN pn-diode as a function of bias voltage at various temperatures. Data taken from Publication III.*

Mn doped pn-diodes were also fabricated. The non-magnetic p-side was lightly doped and the magnetic n-side was heavily doped by Mn. The *I-V* characteristics of the magnetic pn-diodes are shown in Fig. 27. We used the solid state diffusion method to fabricate the Mn doped GaN layer and therefore the crystal quality of the Mn doped GaN was not as good as that of Ham et. al. [89]. The inferior quality of the pn-diode is shown also in the I-V characteristics. In our pn-diodes the rectification ratio was not as good as that of Ham et. al. [89]. No magnetic field dependence of the *I-V* characteristics were observed in our pn-diodes. The possible reasons for that may be the same as that discussed in the case of Mn doped GaAs pn-diodes (Chapter 5.2), where the non-magnetic side is lightly doped. The discontinuity between the layers cannot explain the results either. The reason for ferromagnetism in Mn doped GaN is still unclear, but it is quite obvious that it is not carrier mediated as in Mn doped GaAs and therefore the

absence of ferromagnetism in the depletion region is probably not the cause of the magnetoresistance not been observed. The most probable reason for the absence of MR in Mn doped GaN is that the diffusion current of the lightly doped non-magnetic side dominates the total current.

6 Future Prospects

We have the following preliminary ideas for further studies in semiconductor spintronics

(i) **To fabricate and study room temperature spintronic devices based on Mn doped GaAs.** This can be accomplished, e.g., by growing high T_C magnetic quantum dots and by utilizing the semiconductor layers including these dots as spin emitters. This is an important issue considering the possible spintronic applications.

(ii) **To fabricate and study Mn doped GaAs resonant tunnelling diodes with ZnSe tunnelling barriers.** We will fabricate the ferromagnetic resonant tunnelling diodes with quantum wells based on Mn-doped GaAs using thin insulating ZnSe layers as tunnelling barriers. This is a new structure that has not been realized before in GaAs technology.

(iii) **To fabricate and study Mn doped Spin Esaki-Zener tunnel diodes**: One of the future aims is to study the TAMR effect in Spin Esaki-Zener tunnel diodes in more detail. The study of the tunnelling current gives us information, e.g., about the anisotropy of the electronic structure and density of states near the band edges involved in the spin-dependent tunnelling processes. The high temperature operation is obtained using ferromagnetic quantum dots in the emitter layer.

(iv) **To fabricate and study ferromagnetic MOS capacitors**. By fabricating an insulator layer and metallization on top of a Hall configuration in a ferromagnetic semiconductor, it is possible to accumulate charge carriers in the insulator/semiconductor interface. Since the ferromagnetism in all the new ferromagnetic semiconductors is carrier-induced, the ferromagnetic MOS capacitor allows us to change the magnetic properties of the semiconductor simply by applying the proper gate voltage. This effect has not been studied in Mn-doped GaAs.

(v) **The fabrication of ferromagnetic single electron transistors (SET) using the new FIB technique.** This allows us to study, e.g., the spin-dependent Coulomb blockade effect in SETs [93], whereby we can test some ideas relevant in quantum computing.

7 Summary

Semiconductor spintronics offers several advantages over the present metallic ferromagnetic thin films, such as easier integration with micro- and nanoelectronics, larger magnetoresistive effects, and a possibility to fabricate devices showing current rectification and amplification. However, this requires that the ferromagnetic ordering temperatures can be increased above room temperature. In the present work the most significant result in Mn doped GaN thin film studies was that room temperature ferromagnetism can be achieved using a solid-state diffusion of Mn into GaN. Our studies revealed that despite the fact that the solid state diffusion is quite a simple method, the whole fabrication process is so difficult that it is very hard to produce a large amount of Mn doped GaN samples with exactly the same properties. We have shown that also pn-diodes with n-type Mn-doped layers could be fabricated. This was one of the first Mn doped GaN devices ever. However, due to the fabrication difficulties the quality of Mn doped GaN diodes were not good. Since it was much more straightforward to fabricate various spintronic devices of Mn-doped GaAs, most of the effort in the present work was put into magnetotransport studies in various magnetic diodes made of Mn-doped GaAs, although the highest Curie temperatures in (Ga,Mn)As are below room temperature. The (Ga,Mn)As-based devices studied in the present work included spin Esaki-Zener tunnel diodes and ferromagnetic resonant tunnelling diodes.

The magnetic diode structures were made using low-temperature molecular beam epitaxy and metal-organic vapour phase epitaxy techniques. Ferromagnetism in the grown layers was confirmed by resistivity, Hall-effect and direct magnetization measurements. The magnetotransport measurements revealed - for the first time- a large spin-dependent tunnelling magnetoresistance at low temperatures both in spin Esaki-Zener tunnel diodes and in ferromagnetic resonant tunnelling diodes. More precisely, a tunnelling anisotropy magnetoresistance (TAMR) was observed, which is related to the exchange interaction between the charge carriers and the magnetic atoms and to the dependence of the density of states on the orientation of the magnetization, which can be altered by the external magnetic field. One of the most important findings in this

study was that since the TAMR effect is large at very low bias voltages a low power Spin-Esaki Zener diode could be fabricated from Mn doped GaAs, if the Curie temperature would be high enough. This finding gives hope that some day it is possible to replace some of metallic spintronics devices with semiconductor spintronics devices. Also this study revealed that the magnetic RTD structures can be used to study the valence band structure in Mn doped GaAs.

This study also explains why in some cases the *I-V* characteristics of pn-diodes are not magnetic field dependent even when some part of the device is ferromagnetic. These findings are important in order to fabricate actual magnetic field dependent semiconductor devices. To conclude, this thesis has improved the scientific community's knowledge of magnetotransport properties of semiconductor spintronic devices and shown that it is possible to fabricate devices from diluted magnetic semiconductors that show a large magnetic field dependence.

References

[1] A. Fert, J. George, H. Jaffres, R. Mattana, and P.Seneor, Europhysics News **34** No 6, (2003)
[2] N.F.Mott, Proc.Roy. Soc. A **153**, 699, (1936)
[3] M.N. Baibich, J.M.Broto, A.Fert, F. Nguyen Van Dau, F.Petroff, P. Eitenne, G.Creuzet, A. Friederich and J. Chazeklas, Phys. Rev. Lett. **61**, 2472 (1988)
[4] G.Binasch, P. Grünberg, F.Saurenbach and W.Zinn, Phys. Rev. B. **39**, 4828 (1989)
[5] S.S.P Parkin et. al. Phys. Rev. Lett. **67,** 3598 (1991)
[6] S.Parkin, X. Jiang, C. Kaiser, A. Panchula, K. Roche and M. Samant, Proceedings of the IEEE **91,** 661 (2003)
[7] S.Parkin, C. Kaiser, A. Panchula, M. Rice, B. Hughes, M. Samant and S. Yang, Nature Materials **3,** 862 (2004)
[8] F.Matsukura, H Ohno, A. Shen and Y. Sugawara, Phys. Rev. B **57**, R2037 (1998)
[9] F.Matsukura, H Ohno and Dietl, "III-V Ferromagnetic Semiconductors" in Handbook of magnetic materials chapter edited by K.H.J. Buschow, Elsevier Science, (2003)
[10] H.Munekata, H. Ohno, S. von Molnar, A. Segmuller, L. Chang and L. Esaki, Phys.Rev.Lett. **63**, 1849 (1989)
[11] I.Zutic, J. Fabian and D.Sarma, Review of Modern Physics **76,** 323 (2004)
[12] A.Silva, A.Fazzio, R. Santos and L. Oliveira, Physica B **340-342**, 874 (2003)
[13] H. Ohno, H. Munekata, T. Penney, S. Von Molnar and L. Chang, Phys. Rev. Lett. **68,** 2664 (1992)
[14] H. Ohno, A. Shen , F. Matsukura, A. Oiwa, A. Endo, S. Katsumoto and Y. Iye, Appl. Phys. Lett. **69,** 363, (1996)
[15] J.De Boeck, R. Oesterholt, A. Van Esch, H. Bender, C. Bruynseraede, C. Van Hoof and G. Borghs, Phys. Rev. Lett. **68,** 2744 (1996)
[16] T. Dietl, A.Haury and M. d'Aubigne, Phys. Rev. B **55,** R3347 (1997)
[17] K.Wang, R. Champion, K. Edmonds, M. Sawicki. T. Dietl. C. Foxon, and B. Gallagher, AIP Conf. Proc. **772,** 333 (2005)
[18] A. Nazmul,T. Amemiya,Y.Shuto, S.Sugahara and M.Tanaka, Phys. Rev. Lett. **95,** 017201 (2005)
[19] T. Dietl, H. Ohno, F. Matsukura, J. Cibert and D.Ferrand, Science **287**,1019 (2000)
[20] M.Reed, N. El-Masry, H. Stadelmaier,M. Ritums, M. Reed, C. Parker, J. Roberts and S. Bedair, Appl. Phys. Lett. **79,** 3473 (2001)
[21] S. Dhar, O. Brandt, A. Trampert, L. Däweritz, K.J. Friedland, K.H. Ploog, J. Keller, B. Beschoten and G. Güntherodt, Appl. Phys. Lett. **82**, 2077 (2003)
[22] S.Sonada, S. Shimizu, T. Sasaki, Y. Yamamoto and H. Hori, J. Crys. Growth **237-239,** 1358 (2002)
[23] V.A. Chitta, J. A. Coaquira, J.R. Fernandez, C.A. Duarte, J.R.Leite, D. Schikora, D.J.As, K. Lischka and E. Abram, Appl. Phys. Lett. **85**, 3777 (2004)
[24] N. Lebedeva, S. Novikov, T. Saloniemi and P.Kuivalainen, Physica Scripta **114**, 85 (2004)
[25] T.Dietl, H. Ohno, and F. Matsukura, IEEE Transaction on Electron Devices **54,** 945 (2007)
[26] C.Zener, Phys.Rev. **81**, 440 (1950)
[27] T. Dietl, Semi. Sci. techn.**17**, 377 (2002)
[28] M. Linnarsson, E. Janzen, B. Monemar, K. Kleverman and A. Thilderkvist, Phys Rev. B **55**, 6983 (1997)
[29] J.G. Braden, J.Parker, P.Xiong,S. Chun and N.Samarth, Phys.Rev.Lett. **91,** 056602 (2003)
[30] D.Chiba,N.Akiba, F. Matsukura, Y. Ohno and H. Ohno, Appl. Phys.Lett **77**,1873 (2000)
[31] M. Tanaka and Y. Higo, Phys.Rev. Lett **87,** 026602 (2001)
[32] C. Rüster, C. Gould, T. Jungwirth, E. Girgis, G. Schott, R. Giraud, K. Brunner, G. Schmidt and L.W. Molenkamp, J. Appl. Phys. **97**, 10C506 (2005)
[33] V. Litvinov and V.Dugaev, Phys. Rev. Lett. **86**, 5593, (2001)
[34] G.Das, B. Rao and P. Jena, Phys. Rev. B **68**, 035207 (2003)
[35] T.Graf, S. Goennenwein and M.Brandt, Phys. Stat. Sol. B **239**, 277 (2003)

[36] K. Sato, P. Dederirichs, H. Katayama-Yoshida and J. Kudrnovsky, Physica B **340-342**, 863 (2003)
[37] T.Graf, M. Gjukic, M. Brandt, M. Stutzmann and O. Ambacher, Appl. Phys. Lett. **81**, 5159 (2002)
[38] M. Park,K.Huh, J. Myong, J. Lee, J. Chang, K. Lee, S. Han and W. Lee, Solid State Communications **124**, 11 (2002)
[39] W. Gebicki, J. Strzeszewski, G. Kamler, T. Szyszko and S. Podsliado, Appl. Phys. Lett. **76,** 3870 (2000)
[40] C. Liu, F. Yun, H. Morkoc, Journal of Materials Science:Materials and Electronics **16,** 555 (2005)
[41] S. Pearton, C. Abernathy, G. Thaler, R.Frazier, D. Norton, F.Ren, Y. Park, J. Zavada , I. Buyanova, W.Chen and A. Hebard, J. Phys. Condens.Matter **16**, 209 (2004)
[42] T. Dietl, Journal of Physics:Condensed Matter **19,** 165204 (2007)
[43] P. Edwards and M. Sienko, Phys. Rev.B **17,** 2575 (1978)
[44] E.Abrahams, P.W. Anderson, D.C. Licciardello and T.V. Ramakrishnan, Phys. Rev. Lett. **42,** 673 (1979)
[45] K. Seeger, Semiconductor Physics: An introduction 3rd Edition, Springer-Verglag (1985)
[46] A. Schuhl and D. Lacour, C.R. Physique **6,** 945 (2005)
[47] M.Julliere, Phys. Lett. **54A,** 225 (1975)
[48] L.Brey, C.Tejedor, J. Fernandez-Rossier, Appl. Phys. Lett. **85,** 1996 (2004)
[49] P.Sankowski, P Kacman, J. Majewski and T. Dietl, Phys. Rev. B **75,** 045306 (2007)
[50] R. Giraud, M. Gryglas, L. Thevenard, A. Lemaitre and G.Faini, Appl. Phys. Lett **87,** 242505 (2005)
[51] J. Burton, R. Sabirianov, J. Velev, O. Mryasov and E. Tsymbal, Cond. Matt., 0703345 (2007)
[52] C. Gould, C. Rüster, T. Jungwirth, E. Girgis, G. Schott, R. Giraud, K. Brunner, G. Schmidt and L.W. Molenkamp, Phys. Rev. Lett. **93**, 117203 (2004)
[53] S.Datta and B. Das, Appl. Phys. Lett. **56**, 665 (1990)
[54] N.Lebedeva and P.Kuivalainen, J.Appl.Phys. **93**, 9845 (2004).
[55] H.Ohno, N.Akiba, F.Matsukura, A.Shen, K.Otani, and Y.Ohno, Appl.Phys.Lett. **73**, 363 (1998).
[56] R.Tsu and L.Esaki, Appl.Phys.Lett. **22**, 562 (1973)
[57] P.Kuivalainen and A.Hovinen, J.Phys.D: Appl.Phys. **35**, 48 (2002).
[58] D.K.Ferry and S.M.Goodnick, Transport in Nanostructures, Cambridge University Press, Cambridge, (1997)
[59] J.R.Arthur, J. Appl. Phys. **39,** 4032 (1968)
[60] A.Y.Cho, J. Appl. Phys. **41,** 2780 (1970)
[61] Olli Kilpelä, Juha Sinkkonen and S.Novikov, MBE Growth of Material Systems for Semiconductor Nanostructures, Reports in Electron Physics 15, 1997
[62] M.A.Dubson and D.F.Holcomb, Phys.Rev. B **32**, 1955 (1985).
[63] J.Fabian, I.Zutic, and S.Das Sarma, Phys.Rev.B. **66**, 165301 (2002).
[64] M.E.Flatte and G.Vignale, Appl.Phys.Lett. **78**, 1273 (2001).
[65] M.Kohda, Y.Ohno, K.Takamura, F.Matsukura, and H.Ohno, Jpn.J.Appl.Phys. **40**, L1274 (2001).
[66] E.Jonston-Halperin, D.Lofgreen, R.K.Kawakami, D.K.Young, L.Coldren, A.C.Cossard, and D.D.Awschalom, Phys.Rev.B **65**, 041306 (2002).
[67] P. Dorpe, Z- Liu, W. Roy, V. Motsnyi, M. Sawicki, G. Borghs, J. De Boeck, Appl. Phys. Lett. **84,** 3495 (2004)
[68] M. Ciorga, A. Einwanger, J. Sandowski, W. Wegscheidet and D. Weiss, Phys. Stat. Sol (a) **204**, 186 (2007)
[69] E.E.Mendez, L.Esaki, and W.I.Wang, Phys.Rev. **B33**, 2893 (1986).
[70] R.K.Hayden, D.K.Maude, L.Eaves, E.C.Valadares, M.Henini, F.W.Sheard, O.H.Hughes, J.C.Portal, and L.Cury, Phys.Rev.Lett. **66**, 1749 (1991)
[71] D.E.Bremer, K.Zhang, C.J.Schwarz, S.P.Chau, S.J.Allen, J.P.Ibbetson, J.P.Zhang, C.J.Palmstrom, and B.Wilkins, Appl.Phys.Lett. **67**, 1268 (1995).
[72] A.Haury, A.Wasiela, A.Arnoult, J.Cibert, S.Tatarenko, T.Dietl, and Y.Merle d'Aubigne, Phys.Rev.Lett. **79**, 511 (1997)

[73] N.Akiba, F.Matsukura, Y.Ohno, A.Shen, K.Otani, T.Sakon, M.Matokawa, and H.Ohno, Physica B **256-258**, 561 (1998).

[74] S.Ohya, P. Hai, Y. Mizuno and M. Tanaka, Phys. Rev. B **75**, 155328 (2007)

[75] Nonoyama S. and Inoue J.I 2001 Physica E **10,** 283 (2001)

[76] Mizuta H. and Tanoue T., *The Physics and Applications of Resonant Tunnelling Diodes* Cambridge University press, Cambridge (1995)

[77] K.Sardar, A. Raju, B. Bansal, V. Ventaraman and C.Rao, Solid State Communications **125,** 55 (2003)

[78] Y. Shon, Y. Kwon, S. Yuldashev, Y. Park, D. Fu, D. Kim, H. Kim and T. Kang, J. Appl. Phys. **93**, 1546 (2003)

[79] M. Park,K.Huh, J. Myong, J. Lee, J. Chang, K. Lee, S. Han and W. Lee, Solid State Communications **124**, 11 (2002)

[80] M.Reed, M. Ritums, H. Stadelmaier, M. Reed,C. Parker, S. Bedair and N. El-Masry, Materials Letters **51**, 500 (2001)

[81] M. Overberg, C. Abernathy, S. Pearton, N.Theodoropoulou, K. McCarthy and A. Hebard, Appl. Phys. Lett. **79**, 1312 (2001)

[82] G. Thaler, M. Overberg , B. Gila, R. Frazier, C. Abernathy and S. Pearton, J. Lee, S. Lee, Y. Park, Z. Khim, J. Kim and F.Ren, Appl. Phys. Lett. **80**, 3964 (2002)

[83] K. Huh, M. Ham, J. Myoung, J. Lee, K. Lee, J. Chang, S. Han,H. Kim and W.Lee, Jpn. J. Appl. Phys. **41**, L1069 (2002)

[84] I.Yoon, C. Park, H. Kim, Y. Kim, T. Kang, M. Jeong M. Ham and M. Myoung*,* Journal of Applied Physics **95**, 591 (2004)

[85] G. Thaler, R. Frazier, J. Stapleton, C. Abernathy, S. Pearton, J. Kelly, R. Rairigh, A. Hebard and J. Zavada, Electrochemical and Solid-State Letters **7**, G34 (2004)

[86] H. Yang, H. Al-Brithen, E. Trifan, D. Ingram and A.Smith, Journal of Applied Physics **91**, 1053 (2002)

[87] B. Beschoten, E. Johston-Halperin, D. Young, M. Poggio, J. Girabaldi, S. Keller, S. DenBaars, U. Mishra, E.Hu and D. Awshalom, Phys. Rev. B **63,** 121202 (2001)

[88] I.A.Buyanova, M. Izadifard, W. Chen, J. Kim, F. Ren, G. Thaler, C. Abernathy, S. Pearton, C. Pan, G. Chen, J. Chyi and J.Zavada, Appl. Phys. Lett. **84**, 2599 (2004)

[89] M. Ham, S. Yoon, Y. Park, L. Bian, M. Ramsteiner and J. Myoung, J. Phys:Cond. Matt. **18**, 7703 (2006)

[90] M.L. Reed, M.J. Reed, M.Luen, E. Berkman, F.E. Arkun, S.M.Bedair, J.M.Zavada and N. El-Masry. Phys. Stat. Sol. (c) **2**, 2403 (2005)

[91] M. Li, N. Kim, S. Lee, H. Jeon and T. Kang, Appl. Phys. Lett. **88**, 162102 (2006)

[92] F.Matsukura, H. Ohno, A.Shen and Y.Sugawara, Phys. Rev. B **57**, R2037 (1998)

[93] J. Wunderlich, T. Jungwirth, B. Kaestnet, A.C.Irvine, A.B.Shick, N.Stone, K-Y. Wang, U.Rana, A.D. Giddingns, C.T. Foxon, R.P. Campion, D.A. Willimams and B.L.Gallagher, Phys.Rev.Lett. **97,** 077201 (2006)

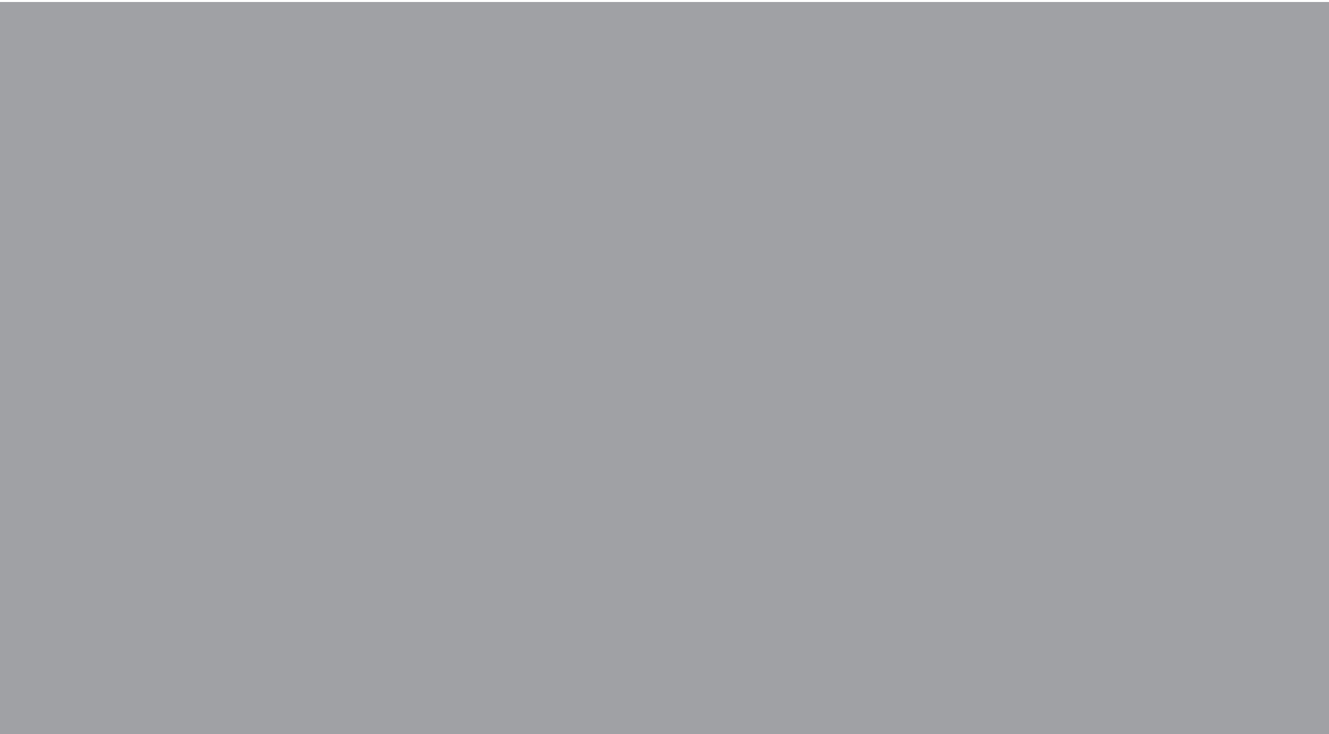

ISBN 978-951-22-9259-2
ISBN 978-951-22-9260-8 (PDF)
ISSN 1795-2239
ISSN 1795-4584 (PDF)